Review

Review on the Adsorption Removal of Contaminants from Wastewater Using Biochar Derived from Agricultural Waste

Pengyun Liu , Luisa Boffa , Giancarlo Cravotto *

Posted Date: 20 October 2025

doi: 10.20944/preprints202510.1476.v1

Keywords: environmental remediation; circular economy; biochar utilization; agriculture waste valorisation; adsorption decontaminant and recovery

 doi:10.20944/preprints202510.1476.v1

Review

Review on the Adsorption Removal of Contaminants from Wastewater Using Biochar Derived from Agricultural Waste

Pengyun Liu, Luisa Boffa and Giancarlo Cravotto *

Department of Drug Science and Technology, University of Turin, via P. Giuria 9, 10125 Turin, Italy

* Correspondence: giancarlo.cravotto@unito.it; Tel: +39-011-670-7183; Fax: +39-011-670-7162

Abstract

Valorisation of agricultural wastes can improve the economic efficiency of crop production while reducing environmental pressures. Owing to its simplicity, high efficiency, low cost, and scalability, the use of biochar as an adsorbent for contaminant removal has been widely studied. Producing biochar from agricultural wastes and applying it to remove contaminants from aqueous and solid matrices, including wastewater and soils, follows the principles of the circular economy and supports environmental remediation and agricultural development. This review summarises adsorption mechanisms, biochar production routes from agricultural wastes, and applications in wastewater treatment. It also evaluates economic performance and environmental impacts, and identifies current challenges and future research directions.

Keywords: environmental remediation; circular economy; biochar utilization; agriculture waste valorisation; adsorption decontaminant and recovery

1. Introduction

Wastewater from various industries poses a tremendous environmental problem and health risk to human beings and water ecosystems [1]. Abundant agricultural wastes are continuously produced globally. It has been reported that the dry biomass production is over 200 billion tons per year around the world, causing a huge agricultural burden [2]. The remediation of wastewater and the appropriate disposal of these agricultural wastes are of great significance to mitigate the aforementioned burden and address these issues.

Adsorption has been a widely applied physicochemical strategy for wastewater purification and the recovery of useful compounds from wastewater [3], owing to the various well-known merits, such as high cost-efficiency, simple design and implementation, high efficiency, robustness, effectiveness, scalability, and sustainability, technically flexible, technologically feasible, and environmentally friendly, free of by-products, simultaneous removal of various contaminants, and resilience against toxic contaminants [4–6]. Generally, the adsorption decontamination performance depends on the preparation processes (*e.g.*, the pyrolysis temperature, gas atmosphere, and heat approaches), the target substrates, the complexity of liquids, the operation properties like dosage of adsorbents, volume of liquids, reaction temperature, content of contaminants, pH of the matrix, contact duration, adsorption mode (batch and column modes), *etc.* [7,8]. Adsorption decontamination favours decreasing the total solids (TS), total organic carbon (TC), total suspended solids (TSS), total volatile suspended solids (TVSS), Total Dissolved Solids (TDS), total organic carbon (TOC), biochemical oxygen demand (BOD), and chemical oxygen demand (COD) of wastewater [8–10]. Meanwhile, the recovered macronutrients such as N, P, and K (in the forms of ammonium, nitrate, phosphate, and potassium salt) from certain types of eutrophication wastewaters like human urine, septic tank wastewater, blackwater, and biogas wastewater via adsorption can be reused to support the growth of crops [11–13]. Similarly, the recovery of phenolic compounds from olive mill

 doi:10.20944/preprints202510.1476.v1

wastewater and N and S from latex industrial wastewater can also be further valued [10,14]. On the other hand, the limitations of adsorption include possible secondary pollution, production of solid waste, requiring extra treatment to degrade the adsorbed contaminants, and so on and so forth [15–18].

Appropriate adsorbents are crucial to ensure excellent adsorption performance [3]. Currently, different adsorbents have been fabricated, such as biochar, activated carbon, zeolites, 2-dimensional materials (*e.g.*, graphene, carbon nanotubes, and MXene), resin, bentonite, covalent-organic frameworks, metal-organic frameworks, and composites, *etc.*[2,19,20]. Among them, biochar has a relatively simple and economic preparation and has been widely used for wastewater remediation. Agricultural wastes have abundant biomass (*e.g.*, lignin, hemicellulose, and cellulose), which is accessible and affordable, and can provide sufficient carbon sources. Agricultural wastes can thus be used as green and non-toxic precursor sources of biochar. The preparation of biochar using agricultural wastes not only favours the valorization of them but also facilitates the reduction of the as-induced environmental and economic burden (*e.g.*, greenhouse gas emissions). Up to now, biochar has been prepared from date seeds [4], almond shells [21], coconut shells [5,22,23], wheat straw [24], rice husks [12,23,25–27], corn wastes [11,28–31], wood wastes [19,32], and rape stalk [33]. The agricultural waste-derived biochar adsorption decontamination is a sustainable and feasible alternative to wastewater remediation [34,35].

Unlike activated carbons, pristine biochar usually possesses a lower surface area and total pore volume, and limited adsorption sites due to poor porosity [8,36–38], followed by poor adsorption ability [10]. Accordingly, the dominant drawbacks of pristine biochar are poor dispersibility (e.g., easy to float and aggregate) [39]. Fortunately, the physicochemical properties (*e.g.*, dispersibility, porosity, separability, mechanical strength, surface area, ionic radius, surface area, electronegativity, and the surface's functional groups, pore size, functional groups, interaction forces, *etc.*) and the adsorption properties (*e.g.*, adsorption capacity, affinity, selectivity), adsorption kinetics, isotherm, and thermodynamics) of a specific biochar can be promoted via activation and modification to improve the porosity, adsorption sites, and surface chemical affinity and interactions [5]. The pristine biochar has been activated using strong acids, strong bases, and metal oxides, and functionalized using various modifiers, via element doping (*e.g.*, N, S, and heavy metals), and surface charge change to better catch target contaminants from wastewater [8,9,24,37,40–43]. It is worth mentioning that the activation, modification, and functional may reduce the cost-effectiveness of biochar preparation.

Herein, based on the background above, this review presents the recent advances of agricultural waste-derived biochar for wastewater remediation via liquid-solid adsorption, mainly focusing on the adsorption mechanisms, biochar preparation and modification, the main outcomes, the economic evaluation, and environmental impacts. Moreover, the future direction and research needs are also recommended to guide and inspire the incoming work. This review follows the principle of the circular economy and waste valorization, providing a deep understanding of agricultural waste disposal and use, presenting the practical application of wastewater decontamination, and contributing to the sustainable development of agriculture and society globally, as well as resource integration and utilization locally.

2. Mechanism of Adsorption Using Biochar

Adsorption refers to the process of the transfer of substrates from liquid matrices to the surface and the subsequent inner porous structure of solid adsorbents through the capillary effect [5,11,44]. The adsorption of contaminants from liquids can occur through the adsorption of individual contaminants (*e.g.*, single solute solution), selective adsorption of target compounds in complex matrices, competitive adsorption between several compounds (*e.g.*, naphthalene and phenanthrene in aqueous solution), and simultaneous adsorption of multiple contaminants (*e.g.*, ammonium-N and nitrate-N in wastewater) [13,30,45]. Generally, both chemical and physical adsorption appear during adsorption, but with different contributions. Chemisorption relates to the precursor and chemical composition of biochar (*e.g.*, the type and amounts of surface functional groups (*e.g.*, –OH, C=O, and

 doi:10.20944/preprints202510.1476.v1

–COOH), the element components), but physisorption depends on the biochar's surfaces and architecture, and weak interaction forces (*e.g.*, Van der Waals forces) [23]. Thus, the chemisorption is usually a single layer and stronger, in which the adsorbed molecules or ions are difficult to escape from the adsorption site. In contrast, the physisorption is commonly multiple adsorptions and relevant weak, thus, allowing the mitigation of the adsorbed compounds into the inner pores [36,37,45,46]. The performance and properties of adsorption decontamination from wastewater depends on the physicochemical properties of biochar (*e.g.*, ash content, hydrophobicity, porous property (micro- or meso- porous), point of zero charge (pH_{pzc}), elements composites (*e.g.*, C/O and C/H ratios), and the surface chemical functional groups), the properties of substrates (*e.g.*, pK_a value, solubility, hydrophobicity, chargeability, electron distribution, and molecular or ion size), the interaction between the components in the bulk liquid and the surface of biochar, and so forth [8,36–38,40,45]. The specific absorption may be the synergistic result of these as-mentioned impacts.

Wastewater has complex components with a variety of molecular sizes, and the entrance of these compounds into the micropores of the biochar is a sufficient condition for effective adsorption. Large-sized compounds can usually be fate adsorbed instead of the smaller-sized counterparts. Nevertheless, the larger molecules can block the micropores, limiting the entrance of the smaller molecules into the smaller pores. Powder biochar usually has a more rapid adsorption than granular biochar due to the biochar size impacts the adsorption rate via limiting the inner mass transfer. However, the biochar size does not affect its total adsorption capacities since it depends on the total specific surface area of biochar [39]. Hydrophobic compounds are more easily adsorbed via hydrophobic interactions than the hydrophilic ones [44]. The large surface area and abundant porous structure (meso- and micro pores) can provide sufficient adsorption sites for the physical and chemical interactions between the biochar and the target compounds [36,37,45,46]. It has been reported that the functional groups may contribute a lot when the biochar has a poor specific surface area [47]. The adsorbent affinity is crucial for high adsorption capacity, regardless of the concentrations of target contaminants [13]. For instance, the smaller the ionic size, the greater its affinity to reactive sites and the faster the mitigation of them, followed by the better adsorption performance [48]. Moreover, many physicochemical interactions are crucial for the effective adsorption of contaminants from wastewater, as listed in Table 1 [2,4,40,49,50]. Specifically, -OH and -NH_2 on the biochar surface are reported to be the dominant groups responsible for the adsorption of anionic dye [50]. The π-π interaction and O-containing groups (*e.g.*, -OH and C=O) on the surface of biochar composites could favour the adsorption of cations through the surface polarization and electrostatic attraction [51,52]. Negatively charged biochar can adsorb ammonium ions via electrostatic attraction and H-bonding between O-containing groups, -OH, C–O, –COOH, and –COC– of biochar and ammonium ions, and phosphate via surface precipitation from urine [11,12,53]. Cations Mg^{2+} and Ca^{2+} in biochar can trap PO_4^{3-} and $H_2PO_4^-$ in liquids via precipitation, while anion Cl- of biochar favours adsorbing PO_4^{3-} via electrostatic forces [11,54,55]. The specific interactions that SiO_2 in biochar can enhance the affinity towards PO_4^{3-} via electrostatic interactions and H-bonding (or ligand exchange) by its -OH group, especially at acid pH [12]. Groups like -OH, -COOH, -Ar, Ar-NH_2 (aromatic amines), R1-CO-N-R2R3 (amides), and -$C_5H_{10}N$- (pyridine) of biochar favour the adsorption of ammonium, nitrate, and phosphate through ion exchange [22]. Biochar can interact with both ammonium- and nitrate-N via electrostatic attraction, ion exchange, and physisorption, and the electrostatic attraction is particularly significant [13]. Additionally, positively charged biochar surfaces can interact with cationic compounds via Coulombic interactions under acidic conditions [56]. The dominant interactions that contributed to the adsorption can be identified via a combined analysis of various adsorption properties and the characterization of biochar before and after adsorption [6,11,57–59].

 doi:10.20944/preprints202510.1476.v1

The mechanisms for the removal of Pb2+, P, AB25 dye, phenol, and atrazine in various wastewater are compiled in Figure 1.

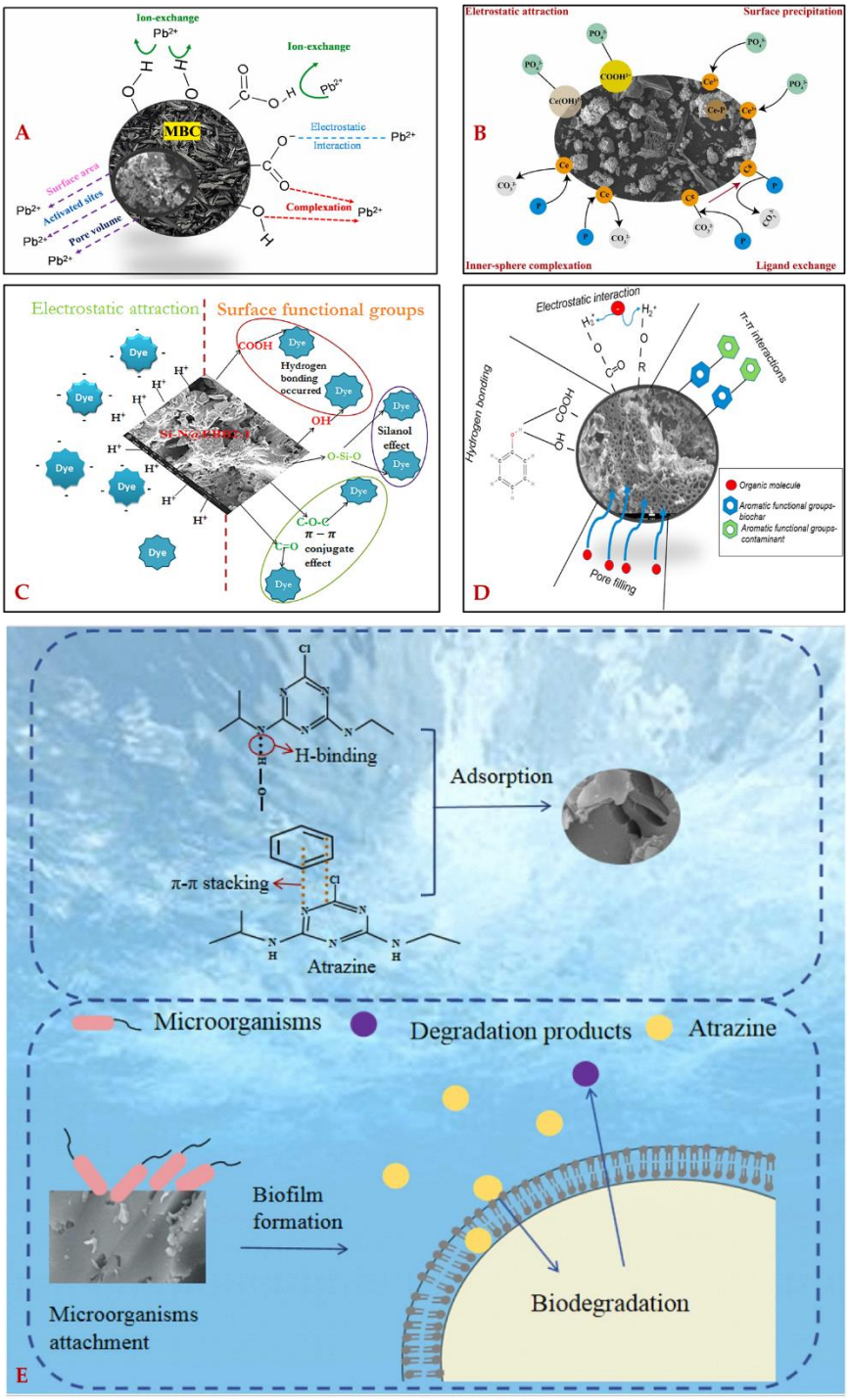

Figure 1. Adsorption mechanisms of: Pb^{2+} by alginate-modified rice husk biochar in wastewater (A). Reprinted from ref. [27]. Copyright (2022), with permission from Elsevier; P by $CeCl_3 \bullet 7H_2O$ modified corn stalks in pig farm wastewater (B). Reprinted from ref. [30]. Copyright (2024), with permission from Elsevier; AB25 dye by silica-nitrogen modified eucalyptus bark biochar in dye wastewater (C). Reprinted from ref. [50]. Copyright (2023), with permission from Elsevier; phenol by date palm frond biochar in municipal wastewater (D). Reprinted from ref. [66]. Copyright (2025), with permission from Elsevier; and possible mechanism of combined adsorption/biodegradation of atrazine by peanut shell-based biochar in simulated wastewater (E). Reprinted from ref. [6]. Copyright (2025), with permission from Elsevier.

 doi:10.20944/preprints202510.1476.v1

Table 1. The mechanisms of the adsorption.

Mechanisms	Illustrations	Examples	Refs.
Precipitation	Contaminants can chemically precipitate via reaction with the liquid solute or biochar surface, and are finally adsorbed on the biochar surface	i) Between Al^{3+}, Fe^{3+}, Ca^{2+}, Mg^{2+}, Zn^{2+}, Cu^{2+}, Pb^{2+}, or Cd^{2+} and OH^- at alkaline conditions ii) Between PO_4^{3-} and Fe-doped biochar to form $Fe_3(PO_4)_2{\cdot}(H_2O)_8$	[10,42,60]
Complexation	Biochar surface's functional groups can act as electron donors or acceptors, interact with metal ions or ammonium ions to produce complexes	i) Between -OH groups and Fe^{2+} ii) Between phosphate and ammonium ion iii) Between –COOH, C=O or –OH with Cr^{6+} iv) Between OH-, C=O or C–OH with Pb^{2+} v) Between $-NH_2$ and Cu^{2+} or Pb^{2+}	[31,40,56]
H-bonding	H-bonding (theoretical bond energies of 4–17 kJ/mol) can be formed via the interaction between the functional groups on the biochar surface (*e.g.*, $-NH_2$ and -OH) with F-, N-, or O- containing molecules	i) Between -OH and ammonium ion or $-NO_2$ ii) Between -OH and -OH or $-NH_2$ iii) Between -COOH and its conjugate acid	[5,13,61]
Electrostatic attraction and repulsion	Electrostatic interaction refers to the formation of ionic bonds between surface-charged biochar and ions or charged molecules. Electrostatic interaction is highly related to the pH of liquids, surface charge of the biochar, and pK_a of the target substrates, which can be limited under high pH	i) Between cationic dye and $-COO^-$ of biochar ii) Between the Si-N of biochar and anionic dyes iii) Between Mn^{2+} and -OH, -COOH, or C=O of biochar iv) Between PO_4^{3-} and nitrate or nitrite of biochar v) Between the same ions on the biochar surface and in liquids	[5,50,62]
π-π electron donor–acceptor interaction	π-π interactions (theoretical bond energies of 4-167 kJ/mol) are weak non-covalent bonds, referring to interactions between groups with π electron systems (*e.g.*, -Ph, -C=C-, C=O, -COOH, -OH, and C-O) of the biochar surface and the target compounds.	i) Between -Ph of biochar and the enone structure of tetracycline ii) Between -OH or -COOH of biochar surface and -Ph of phenolic compounds	[2,6,20]
Pore-filling	Pore filling is a physisorption process, referring to the substrate being adsorbed and concentrated on biochar's pore, depending on the properties of biochar (*e.g.*, porosity) and the substrate (*e.g.*, polarity)	i) Extensively occurs during various porous biochar involved adsorption	[42,63]

 doi:10.20944/preprints202510.1476.v1

Ion exchange	Ion exchange refers to the exchange of ions between the biochar surface and the charged substrate in liquid	i) Between the SiO_2 of biochar and ammonium-N ii) Between Ca^{2+}, Na^{+}, or K^{+} of biochar and Hg^{2+} iii) Between -COOH, -OH, or -FeOOH of biochar with Cr^{6+}	[12,31,64]
Ligand exchange	Ligand exchange refers to the original ligand of a coordination compound of biochar being selectively substituted by other ligands in liquids, which is limited at high pH	i) Between -OH of biochar and PO_4^{3-} in liquids ii) Between S- or O- containing groups of biochar with Cd^{2+} in liquids	[30,52,65]
Hydrophobic interaction	Hydrophobic interaction refers to the interaction between aromatized, graphitized layers or the hydrophobically modified surface of biochar and hydrophobic substances	i) Extensively occurs between the hydrophobic surface of biochar and hydrophobic compounds ii) Between oleic acid-modified activated biochar and naphthalene	[40,46]
Redox effects	Redox effects occur between biochar surfaces with oxidation or reduction capabilities and substrates in liquids	i) [Adsorbent]-Fe^{2+} + CrO_4^{2-} + $4OH^{-}$ + $4H_2O \rightarrow 3\ Fe(OH)_3$ +$Cr(OH)_3$	[39]
Van der Waals forces	Van der Waals forces, a weaker electrostatic interaction than H-bonding, refer to non-directional and unsaturated interactions between the biochar surface and substrates in liquids	i) Between the biochar surface and neutral creatinine, urea, or uric acids	[12]

Various conditions also influence the adsorption, such as initial contaminant concentration, connection time, dosage of biochar, pH and temperature of the adsorption system, and co-existing ions. Generally, high initial concentrations favour adsorption due to the large concentration gradient and high driving force lead to great interphase mass transfer, intrapore molecule diffusion, and improved affinity of biochar towards the target compounds, followed by rapid adsorption with high capacity [1,19,48,65,66]. At the initiation of adsorption, the process proceeds rapidly, attributed to the sufficient and accessible adsorption sites, a high concentration difference driving force, and low diffusion resistance. With prolonged connection time, the adsorption will gradually slow down due to the limited adsorption sites and low mass transfer and molecular diffusion. Eventually, a dynamic adsorption-desorption equilibrium will be reached, where the total adsorption capacity becomes stable, and the adsorption site may continue the empty-occupy cycle, and the adsorbed compounds might influence the remained ones in liquids via electrostatic repulsion, size exclusion, or other weak interactions [1,2,10,23,52,66]. High dosages of biochar do not always favour adsorption. Appropriate dosages can not only offer enough surface adsorption sites and ensure economical and fast operation but also avoid the biochar congestion [19,30,31,52]. The influence of pH on adsorption is complex. For biochar, the pH of adsorption systems can change the types and distribution of biochar's surface charge via altering the zeta potential of biochar relative to its pH_{pzc} and the dissociation of chemical groups of biochar's surfaces, and thus affecting the electrical interactions with the target substrates in liquids [1,5,56]. It has been reported that the alternation of biochar's surface charge can promote

 doi:10.20944/preprints202510.1476.v1

its adsorption selectivity [13]. For the target substances (*e.g.*, dyes, TC, phosphorates, ammonium, and Fe ions), especially the amphoteric compounds, pH can change their existence form (molecule or ion) in liquids, and thus impact their affinity with biochar [6,19,30,47]. Usually, acidic conditions (pH 5-6) favour metal sorption, whereas alkaline conditions facilitate the organics and PO_4^{3-} sorption [60,67]. Under very acidic conditions, competitive adsorption between target compounds (*e.g.*, metal ions and NH_4^+) and H^+ and electrostatic repulsion will occur, limiting the adsorption [19,51,52]. Under alkaline conditions, organics are highly ionized, allowing high mitigation and diffusion of them [67]. Alkaline conditions favour biochar adsorption by promoting their surface negative charge density and enhancing the induced electrostatic interaction [47,60]. Alkaline conditions also favour cation adsorption via electrostatic attraction, surface complexation, and precipitation, but inhibit anion adsorption via the competitive adsorption of OH^- ion and electrostatic repulsion [23]. High temperature is conducive to endothermic adsorption, while low temperature is conducive to exothermic adsorption. However, high temperatures can decrease the adsorption interaction and intensify molecular motion, which may result in the desorption of substances [1,19]. The effect of temperature can be detailed via the thermodynamic investigations [36,37,46]. The co-existing ions (*e.g.*, Cl^-) change the ionic strength of the liquids, impacting the adsorption via the salting-out effect, molecular dissociation, competitive adsorption, and electrostatic screening effect [13,52]. Thus, the optimal adsorption conditions are crucial for the desired adsorption performance.

The static adsorption behaviour and properties can be deconstructed using kinetic, thermodynamic, as well as isotherm models. The kinetic study favours clarifying the rate-control step (*e.g.*, chemical adsorption and mass transfer) during adsorption [4,19]. The most used kinetic models are the pseudo-first order (PFO), the pseudo-second order (PSO), and the Elovich kinetic models [36,68]. In case of high-concentration substances, the PFO model is more suitable to describe the adsorption processes than the PSO model [69]. Adsorption isotherms describe the adsorption layer characteristics and the relationship between the substrates and biochar (*e.g.*, the highest adsorption capacity, physi- or chemi-sorption, and adsorbent surface properties) [36,68]. The frequently applied adsorption isotherm models are the Langmuir, the Freundlich, the Temkin model, the Redlich-Peterson, and the Dubinin-Radushkevich isotherm models [1,2,19,56]. Moreover, Vaishali et al. studied the competitive adsorption of methyl paraben, carbamazepine, ibuprofen, and triclosan using Multicomponent Freundlich and Langmuir isotherm models [13]. Adsorption mechanisms (*e.g.*, rate-limiting steps) can commonly be clarified via the Weber and Morris model (also known as the intraparticle diffusion model) and the Boyd model (also known as the film diffusion model) [20]. Moreover, the adsorption thermodynamic properties can be determined using the Arrhenius formula and the Van't Hoff equation with considering the effect of adsorption temperature [19,36,37]. The difficulty of the adsorption can be evaluated using Gibbs free energy ($\Delta G°$), enthalpy ($\Delta H°$), and entropy ($\Delta S°$) [52]. On the other hand, the column adsorption (also known as dynamic adsorption) processes can be described using the Thomas and the Adams–Bohart breakthrough curve models. The higher the column height and the lower the flow rates, the more adsorption sites and the sufficient the axial diffusion and mass transfer, followed by the longer the breakthrough time [52,65].

The equations for calculating individual and competitive adsorption capacities of biochar and various models are compiled in Table 2. It is worth mentioning that these models can only speculate on the adsorption mechanism, which should be verified and analyzed in combination with the practice adsorption investigations and biochar characterizations.

 doi:10.20944/preprints202510.1476.v1

Table 2. The models and equations in biochar adsorption.

Models and equations		Nomenclature	Illustrations	Refs.
Individual adsorption capacity	$q_e=\frac{(C_0-C_e)V}{m}$	C_0- the initial concentration of substrate C_e (mg/L)- the equilibrium concentration q_e (mg/g)- the equilibrium adsorption amount V (L)- the reaction volume m (g)- the biochar's mass	Used for calculating the adsorption capacity of a single substrate	[7]
Competitive adsorption capacity	$C_A=\frac{k_{B\text{-}2}d_{\lambda_A}-k_{B\text{-}1}d_{\lambda_B}}{k_{A\text{-}1}k_{B\text{-}2}-k_{A\text{-}2}k_{B\text{-}1}}$ $C_B=\frac{k_{A\text{-}1}d_{\lambda_B}-k_{A\text{-}2}d_{\lambda_A}}{k_{A\text{-}1}k_{B\text{-}2}-k_{A\text{-}2}k_{B\text{-}1}}$	C_A and C_B (mg·L^{-1})- the concentrations of A and B, respectively $k_{A\text{-}1}$, $k_{A\text{-}2}$, $k_{B\text{-}1}$, and $k_{B\text{-}2}$- the calibration constants for the A and B at their characteristic sorption wavelength (*i.e.*, λ_1 and λ_2) d_{λ_A} and d_{λ_B}- the optical densities of λ_1 and λ_2, respectively	Used for calculating the adsorption capacities of multiple substances	[45]
PFO kinetic model	$\ln(q_e-q_t)=\ln q_e-\frac{K_1}{2.303}t$	q_t (mg/g)– adsorption capacity at time t K_1 (min^{-1})– the PFO rate constant	Describing the alteration rate of adsorption capacity over time is positively correlated to the gradient between the q_e and q_t (or instant free sites)	[36]
PSO kinetic model	$\frac{t}{q_t}=\frac{1}{K_2q_e^2}+\frac{t}{q_e}$	K_2 (g/(mg min)) – the PSO rate constant	Describing the adsorption rate positively relates to the improved useful adsorption sites, while chemisorption is dominant and related to strong interaction (valency forces) of the target contaminant and biochar	[37]
Elovich model	$q_t=\frac{1}{\beta}\ln(\alpha\beta)+\frac{1}{\beta}\ln(t)$	α (mg/(g min))– the initial sorption constant β (g/mg)– the initial desorption constant	Describing initial heterogeneous surface chemisorption.	[68]

 doi:10.20944/preprints202510.1476.v1

Langmuir isotherm model	$\frac{C_e}{q_e}=\frac{1}{q_m}C_e+\frac{1}{q_m K_L}$	q_m (mg/g)– the maximal adsorption capacity K_L (L/mg)– the Langmuir constant related to the adsorption free energy $R_L=\frac{1}{1+K_L C_0}$	Describing monolayer physisorption occurs at a specific homogeneous surface with fixed active site amounts and the same energy, and free of interactions among the uptake molecules and lateral interactions. R_L values between 0-1 suggest favorable adsorption	[40]
Freundlich isotherm model	$q_e=K_F C_e^{\frac{1}{n}}$	K_F (L/mg)–adsorption bonding energy (or affinity parameter) 1/n– the adsorption intensity coefficient, indicating the adsorption driving force magnitude	Describing non-ideal and reversible multilayer adsorption at heterogeneous surface sites, with exponentially decreased energy distribution, uneven adsorption enthalpy distribution, and improved surface coverage 0<1/n<1 (or high K_F values) suggests favorable adsorption and high adsorption ability 1/n>1 suggests unfavorable adsorption n=1 suggests linear adsorption n=0 suggests unfavorable and irreversible adsorption	[70]
Temkin isotherm model	$q_e=(\frac{RT}{b_T})ln(K_T C_e)$	b (mol²/J²)- the adsorption free energy b_T (kJ/mol)- the Temkin constant K_T (l/g)- the equilibrium binding constant T (K)- the temperature of the adsorption system	Describing the chemisorption on uneven surface involves adsorbent–adsorbate interaction and the non-uniform and linear decreased adsorption heat, neglecting the impact of extreme concentration values	[50]
Redlich–Peterson isotherm models	$q_e=\frac{K_R C_e}{1+a_R C_e^{\theta}}$	K_R (L/g) - Redlich-Peterson constant a_R (L/mg$^{(1-1/A)}$- Redlich Peterson constant θ- the exponent reflecting the heterogeneity of the adsorbent	Describing the combined characteristics of both the Langmuir and the Freundlich models	[10]

 doi:10.20944/preprints202510.1476.v1

Dubinin-Radushkevich isotherm model	$lnq_e = -K_{DR}R^2T^2\left(1+\frac{1}{C_e}\right)+lnq_{DR}$ $E_S = \frac{1}{\sqrt{2K_{DR}}}$	K_{DR} (mol²/J²)- a constant indicating the adsorption energy q_{DR} (mg/g)- the adsorption capacity E_S (kJ/mol) – a value crucial to clarify the adsorption mechanisms	Describing whether the adsorption follows the micropore filling mechanism, which is a more general monolayer adsorption model than the Langmuir type. $E_S < 8$ suggests a physisorption $8 < E_S < 16$ suggests an adsorption related to ion exchange $E_S > 16$ suggests a chemisorption	[9]
Weber and Morris model	$q_t = K_P t^{\frac{1}{2}} + C$	K_P (mg/(g min$^{1/2}$))– the intraparticle diffusion constant C – a constant related to the boundary layer thickness	Describing three-step adsorption, *i.e.*, the transfer of adsorbed substrates from liquids to the boundary layer, from the boundary layer to the biochar surface, and intraparticle diffusion into biochar. If the linear plot passes through the origin, intraparticle diffusion is the only controlling step. High intercept favors the adsorption	[57]
Boyd model	$-\ln\left(1-\frac{q_t}{q_e}\right) = K_{bf}\,t$	K_{bf} (1/min)– liquid-film diffusion constant	Describing the transfer of adsorbed substrates from the liquids to the surface of the biochar. If the linear plot passes through the origin, film diffusion is the only rate-limiting step	[34]
Thomas breakthrough curve model	$\frac{C_t}{C_0} = \frac{1}{1+\exp\left(\frac{k_{Th}q_0 m}{v} - k_{Th}C_0 t\right)}$	k_{Th} (mL/(min mg))– the Thomas rate constant q_0 (mg/g)– the adsorption capacity v (mL/min)– the feed flow rate	This model is derived from the Langmuir isotherm and PSO models, describes the adsorption mainly being controlled by interface mass transfer instead of chemical interactions, and is commonly used to predict the column adsorption performance of biochar	[68]
Adams–Bohart breakthrough curve model	$\frac{C_t}{C_0} = \exp\left(k_{AB}C_0 t - k_{AB}N_0\frac{z}{U_0}\right)$	k_{AB} (L/(mg min))– the kinetic constant N_0 (mg/L)– the saturation concentration z (cm) – the bed depth of the fixed bed column	Describing the adsorption rate is limited by external material transfer, the adsorption balance does not achieve instantaneously, and the	[52]

 doi:10.20944/preprints202510.1476.v1

		U_0 (cm/min)– the superficial velocity	adsorption capacity of the adsorbent is proportional to the adsorption kinetics, which is generally used to explain the relevance between C_t/C_0 and t in the initiation of breakthrough curves ($C_t/C_0 \leq 0.15$)	
Arrhenius formula	$\ln K_2 = \ln A - \frac{E_a}{RT}$	A- the Arrhenius constant R (8.314 J/(K mol))- the universal gas constant	Describing the effects of temperature on adsorption	[37]
Van't Hoff equation	$lnK_d^\theta = \frac{q_e}{C_e}$	lnK_d^θ (L/g) is the distribution coefficient	Describing the effects of temperature on adsorption	[5]
Gibbs free energy	$\Delta G^0 = -RTlnK$ $K = \frac{C_e}{q_e}$	ΔG^0 (kJ/mol)- the Gibbs free energy	Negative ΔG° values identify spontaneous adsorption. ΔG° values in the range of 0-20 kJ/mol suggest physisorption	[66]
Enthalpy and entropy	$lnK = \frac{\Delta S^0}{R} - \frac{\Delta H^0}{RT}$	ΔS^0 (kJ/mol)- the adsorption enthalpy ΔH^0 (kJ/mol)- the adsorption entropy	Negative ΔH° values identify exothermic adsorption. ΔH value (67.74 kJ/mol) shows chemisorption. ΔH° of 40-800 kJ/mol and (2.1-40 kJ/mol identify chemisorption and physisorption, respectively. Negative ΔS° values indicate the entropy-decreasing adsorption, high orderliness, low molecule colliding, and low intramolecular and intermolecular degrees of freedom of adsorbed molecules	[20]

 doi:10.20944/preprints202510.1476.v1

3. Preparation and Characterization of Biochar from Agriculture

Biochar, porous C-rich material, can be prepared via high-temperature (200–1700°C) pyrolysis of biomass (*e.g.*, lignocellulose) under anaerobic, O_2-limited or O_2-free atmospheres, such as inert gas and vacuum environments [9,10,20,23,60]. In general, biochar has a rough surface, irregular shape, condensed structure, relatively high pore volume and surface area (lower than activated carbon), density, greatly aromatized and graphitized architectures, and abundant surface functional groups (*e.g.*, -OH, -COOH, -NH_2, and C=O)[24,30,40,71]. Biochar's C contents can be identified as high (≥60%), middle (30%-60%), and low (10%-25%) [13,23,50]. Biochar has the strengths of rich C content, stable C structure, abundant precursors, sustainable production, renderability, high cost-effectiveness, convenient modification and surface functionality, high catalytic activity and thermal stability, high accessibility for dissolved pollutants, and can remove both inorganic metal ions and organic contaminants [20,39,42,71]. The weaknesses of biochar include poor affinity, low selectivity, and small co-adsorption capacity [13,71].

Various approaches have been developed for the biochar preparation, including conventional high-temperature carbonization [32,42,72], microwave-assisted high-temperature carbonization [8,33,73], strong acid carbonization [74], conventional hydrothermal carbonization [8,37], and microwave-assisted hydrothermal carbonization [8] using different agricultural wastes as precursors at present. Different agricultural wastes have different elemental compositions and thus exhibit different properties [9]. In general, these agricultural wastes require pre-treatment to clean and dry the material, and to small and uniform the size, as shown in Figure 2 [4]. Conventional carbonization is often operated at high temperature under inert gas atmosphere or vacuum conditions at open or closed systems using a muffle furnace, tubular furnace, curable tube, heat pipe reactor, top-lit updraft two-barrel furnace, portable charring kiln, microwave oven, and so forth [13,14,20,24,42,60]. According to the preparation conditions, pyrolysis can be divided into slow pyrolysis (300-700°C, several hours, 35-50 wt% of yields), fast pyrolysis (400-600°C, <10 s, <30 wt% of yields), and flash pyrolysis (about 1000°C, <3 s, <20 wt% of yields) [60]. Unlike pyrolysis under atmospheres, vacuum decomposition induces faster volatile removal, slighter pore blockage, lower loss of surface groups, and shorter combustion duration, followed by greater yields and properties of the biochar [1]. Hydrothermal carbonization is usually performed by mixing the precursor with less solvent (*e.g.*, distilled, acidified, or alkaline water and or organic reagents), subsequently reacting under high temperature (80–250°C) and pressure (2–6 MPa) [8,37]. Microwave heating can assist both the regular and hydrothermal carbonization owing to the distinct heating ways [8,36,37,46,75]. These approaches have been described in detail in our previous works [8,36,37,46]. Additionally, the molten salt method has also been used, in which micro-pores are formed via the partial oxidation of components under high temperature and air atmospheres, while larger pores are formed thanks to the etching and the template impacts of the molten inert salts [51]. Among the above-mentioned approaches, the conventional high-temperature carbonization has been widely applied for biochar preparation [43,76]. During the preparation processes, the biomass undergoes melting, softening, vesicle formation, and decomposition with gas emission [51]; the light organics of biomass precursors are highly reacted and disrupted via volatilization [23]; the hemicellulose and cellulose usually decompose at 200-300°C and 300-400°C, respectively [51]; the existing metal components may accelerate the pyrolysis of the biomass and improve the porosity of biochar [12,77]; the oxidation induces low ash components and high gas emission under air atmosphere [56]; the pH_{PZC} value can be increased (due to the elimination of acidic O-containing groups, like -COOH, -OH, and R–CH=O), and yields of C and biochar can be improved (due to low oxidation) under high temperatures and limited O_2 atmosphere [12,47]; the exterior of biomass usually suffers more rapid decomposition compared to the inside part, leading to visible cracks and the exposure of the inner Si-containing structure [67]; the aromatic groups can be formed via the condensation and pyrolysis of lignocellulosic [35]; and the C yield and ash fractions relate to the lignocellulose contents in the

 doi:10.20944/preprints202510.1476.v1

precursors [23]. Moreover, the porous structure of biochar can be blocked by tarry and alkaline metal components during the biomass preparation [40].

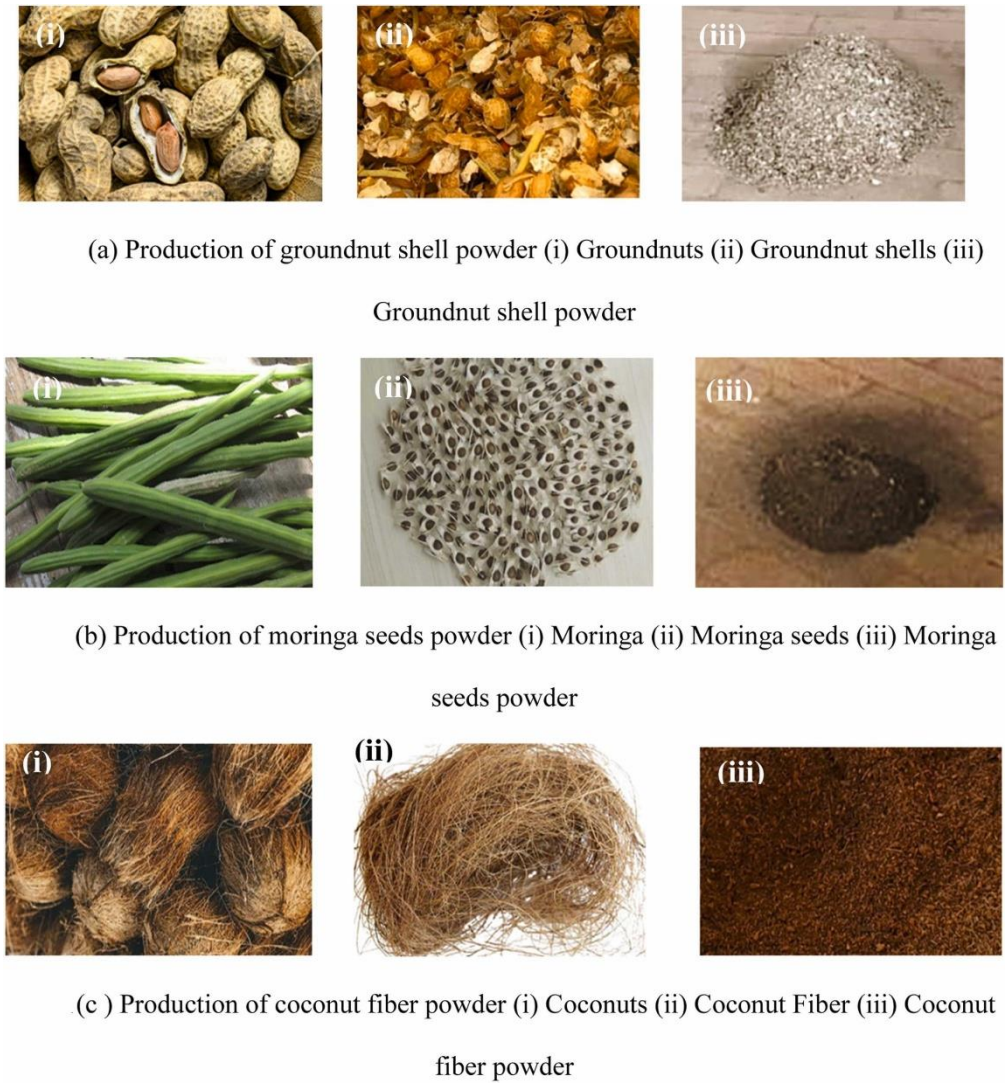

Figure 2. Pretreatment of agricultural wastes for the preparation of biochar. Reprinted from ref. [7]. Copyright (2025), with permission from Elsevier.

Precursor type, carbonization strategies, heating approaches (temperature, way, rate, and holding duration of heating), and carbonization atmosphere (*e.g.*, air, N_2, Ar, vacuum, and adiabatic conditions) can influence the physicochemical and structural properties of biochar [14,24,56,60]. Various precursors include different metals, inorganic, and organic components, impacting the pH_{pzc} value, morphology, and C/H and C/O ratios of biochar [47]. Wood-based biochar is usually reported to exhibit higher stability and better surface and adsorption properties than the others [57]. Alkali metals in the precursor help broaden the biochar lattice and the pore size [41]. Mg and Ca remaining in biochar after pyrolysis favour cation adsorption via ion exchange [54,55]. SiO_2 and its content in precursors, especially for rice husk, have been reported to promote the texture, architecture, and porosity of biochar [12,67]. SiO_2 can also react with H_2O to produce Si-OH on the biochar's surface, which favors adjusting its surface charge at different pH values [50]. Biochar's hydrophobicity, aromaticity, and graphitization improve with the augmented carbonization temperature [40]. On the other hand, these metal components may induce the reduction of biochar's surface area and the obstruction of its pores [35]. Low carbonization temperatures (< 400°C) lead to low specific surface area (<10 m^2/g), but favour protecting the functional groups, increasing the hydrophilicity of biochar (due to the preservation of O-containing groups) and the removal of polar or inorganic contaminants

 doi:10.20944/preprints202510.1476.v1

via surface functional group-induced precipitation, ion exchange, and electromagnetic gravity [22,47,60]. In contrast, raising the temperature (500-700°C) highly improved the surface area (>100 m^2/g), pore volume, and porosity owing to the rapid generation of volatile substances (*e.g.*, H_2, CO, and CH_4), the sufficient discharge of them, decomposition of by-products in pores (*e.g.*, tar oil), and the occurrence of aromatic condensation [12,41,66]. Nevertheless, high carbonization temperatures are not always beneficial. Excessive temperature (>700°C) could decrease the surface functional group (*e.g.*, C=O, -COOH, -OH) content via dehydration and deoxygenation, reduce the surface area and yield of biochar, increase the alkalinity of biochar (due to the removal of acidic groups), rise the pH_{pzc} of biochar (since the dehydration and decarboxylation and the presence of basic carboxylate and hydroxide groups) intensifies), disrupt the biochar's structure, and limit the subsequent adsorption ability [12,13,51,57,66]. The C content of biochar can be improved via H_2SO_4 and sonication treatment in sequence [74].

The physicochemical processing, including activation, modification, and functional of biochar, favours the improvement of its surface and pore properties [13,40]. In general, biochar can be chemically and physically activated using KOH, K_2O, NaOH, $NH_3 \cdot H_2O$, $MgCl_2$, $ZnCl_2$, $CaCl_2$, HNO_3, H_2SO_4, H_3PO_4, HCl, CO_2, steam, *etc.* [8,9,24,37,40–42]. Compared to chemical activation (450-900°C), physical activation commonly requires a higher temperature and longer duration [41]. Chemical treatment can increase the pH_{pzc} through protonating the functional group and removing carbonates and hydroxide in biochar [13]. Particularly, activation using $NH_3 \cdot H_2O$ can trigger the dehydration, decarbonization, and dehydrogenation of substances containing C=O, changing the H/C and C/O fractions and introducing basic N-containing groups [71]. Activation using CO_2 can induce the oxidation of biochar and introduce O-containing groups [77]. Nevertheless, the use of these activators could cause negative environmental effects and low cost-effectiveness. For instance, $ZnCl_2$ is known as a toxic activator, which may induce secondary pollution and pose potential environmental risks. Biochar has been functionalized using a variety of modifiers, like CS_2, sodium alginate (Figure 3), cellulose, chitosan, coal fly ash, inorganic elements (*e.g.*, N and S), and transition metal (*e.g.*, La) and their salts (*e.g.*, Fe_3O_4, as shown in Figure 3) [5,27,31,39,52,77,78]. Specifically, incorporating sodium alginate in biochar can enhance metal cations adsorption via coordination interactions [79]. Coal fly ash is conductive to promoting the surface aromaticity and hydrophobicity, and reducing C=O but protecting R1(R2)C=O groups [77]. S-doping is conducive to immobilizing the metals and introducing functional groups (*e.g.*, S^{2-} and SO_3^{2-}) [52]. N-doping can enhance the surface polarization and electrostatic attraction of metal cations [51,52]. Metal-doping into biochar can decrease the electronegativity and alter the surface charge distribution, and thus improve its affinity [30]. La-doping in biochar can improve the specific affinity for PO_4^{3-} [65]. Fe-doping could promote various properties of biochar, such as surface texture, magnetism, surface charge density, mechanical strength, thermal stability, redox ability, *etc.* [39,60]. Ca-doping contributes to broadening the pH suitability of biochar, as well as improving the biochar decomposition, improving the porosity, and supporting the Fe-doping [60,80]. However, the modifiers may lead to some adverse effects on biochar, *e.g.*, the blockage of pores, the decrease of the surface area, and the reduction of the economic efficiency of biochar [52]. In addition, recyclability and regeneration of biochar are crucial for evaluating its stability, economic efficiency, sustainability, feasibility, and practicality [1]. Most of the developed biochar or their composites exhibit excellent reusability, with low reduction of the adsorption capacity after at least three adsorption-desorption cycles [5]. The decrease in adsorption capacities of biochar after several adsorption-desorption cycles has been frequently reported, which can be attributed to the inactivation of certain adsorption sites owing to the reduced surface area and pore obstruction after thermal processing, the disruption of surface functional groups and the loss of some functional elements (*e.g.*, N, S, and mental) by solvents and under high temperature processing, incomplete desorption due to the strong bonding, and the interference of other compounds in wastewater [13,31,38,52,81]. The consumed biochar can be regenerated via high-temperature treatment (*e.g.*, 150°C [13]) and solvent elution (*e.g.*, 30% EtOH, distilled water, 0.1 M EDTA, HCl,

 doi:10.20944/preprints202510.1476.v1

NaOH, HNO_3, and H_2SO_4 solutions), which favours the valorization of waste biochar and the removal of the secondary pollution risk from the enriched contaminants in biochar [13,20,23,24,31,37,66,74].

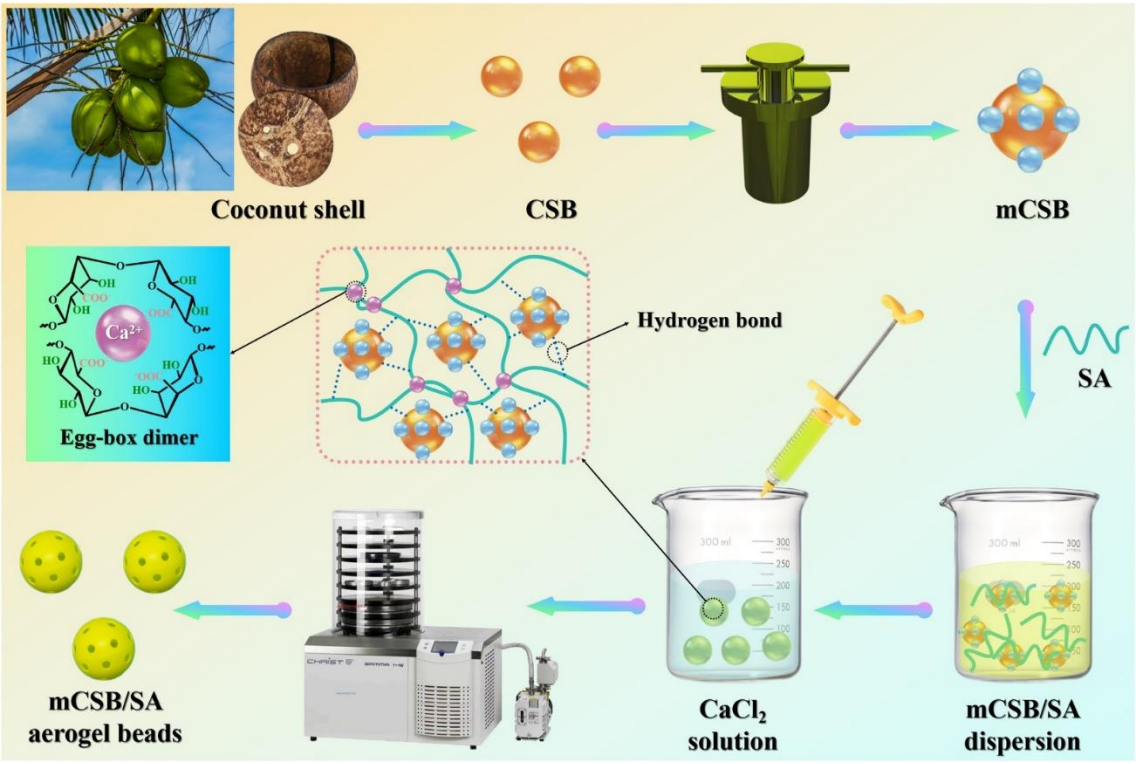

Figure 3. The fabrication of Fe_4O_3-modified coconut shell biochar (mCSB)/sodium alginate (SA) composite aerogel beads. Reprinted from ref. [5]. Copyright (2025), with permission from Elsevier.

Usually, the physicochemical properties of biochar can be clarified using Fourier-transform infrared spectroscopy (FT-IR), Brunauer–Emmett–Teller (BET) surface analysis, scanning electron microscopy (SEM) characterization, energy-dispersive X-ray spectroscopy (EDS, also known as elemental analysis), zeta potential measurement, X-ray diffraction (XRD), X-ray photoelectron spectroscopy analysis, and Thermogravimetric Analysis (TGA) [8,36,46]. FT-IR analysis of biochar before and after adsorption favours clarify the chemical interaction and functional groups that contribute to the effective adsorption, as well as the adsorption mechanism. BET analysis offers the porosity information of biochar, including specific surface area, pore diameter distribution, micropore, mesopore, and total pore volumes. The pore size in biochar can be divided into micro- (<2 nm), meso- (2-50 nm), and macro-pores (>50 nm) [36,37,47,82]. Mesopores of biochar are of great importance for sufficient active sites, ensuring better diffusion and mass transfer [66]. SEM images present the morphology and texture of the biochar surface, such as porosity, granularity, roughness, construction (*e.g.*, multi-layer, spherical, tube, and core-shell structure), *etc.* EDS analysis can deconstruction the element composites of the biochar surface, especially useful when combined with the SEM analysis. Zeta potential analysis facilitates the illustration of the pH effects and the adsorption mechanism (*e.g.*, electrostatic interaction between the surface of biochar and substrate molecules) [6]. The pH_{PZC} value relates to the pH of liquids (pH_L) where biochar's surface is free of charge. Biochar's surface is negatively charged as $pH_L > pH_{PZC}$, and vice versa [47]. Combining various characterizations with the adsorption properties helps to interpret the adsorption mechanisms comprehensively. XRD can identify the crystal phase composition of biochar. Crystallinity can affect biochar's reactivity, porosity, and stability, thereby impacting its performance in various environmental and agricultural applications [30,57]. XPS analysis can determine the atomic composition, contents, valence, bonding patterns, and surface properties in the biochar [1,6,12]. TGA analysis was conducted to evaluate the thermal stability and degradation behavior of the biochar

 doi:10.20944/preprints202510.1476.v1

over a range of temperatures. It provided insights into temperature-dependent changes in weight and helped understand the decomposition patterns of the biochar under different conditions [57].

4. Application of Biochar Adsorption of Wastewater

Agricultural waste-biochar adsorption is a low-cost and effective wastewater remediation strategy, able to remove different contaminants, including dye, antibiotics, pesticides, pharmaceutical residues, heavy metal ions, nutrient substances, and organic carbon, as well as improve the wastewater quality (*e.g.*, turbidity, chroma, smell, pH value, and toxicity) [35]. The adsorption capacity of biochar is commonly lower in wastewater than in clean water due to the competitive adsorption among the target compounds with other contaminants, caused by the complex composites of wastewater [59]. Thus, biochar has been combined with other materials, *e.g.*, poly(*N*-hydroxyethylacrylamide) hydrogel, to achieve better decontamination performance of wastewater [3,53,83,84]. A conceptual framework for valorizing date seeds into biochar for pesticide removal is shown in Figure 4.

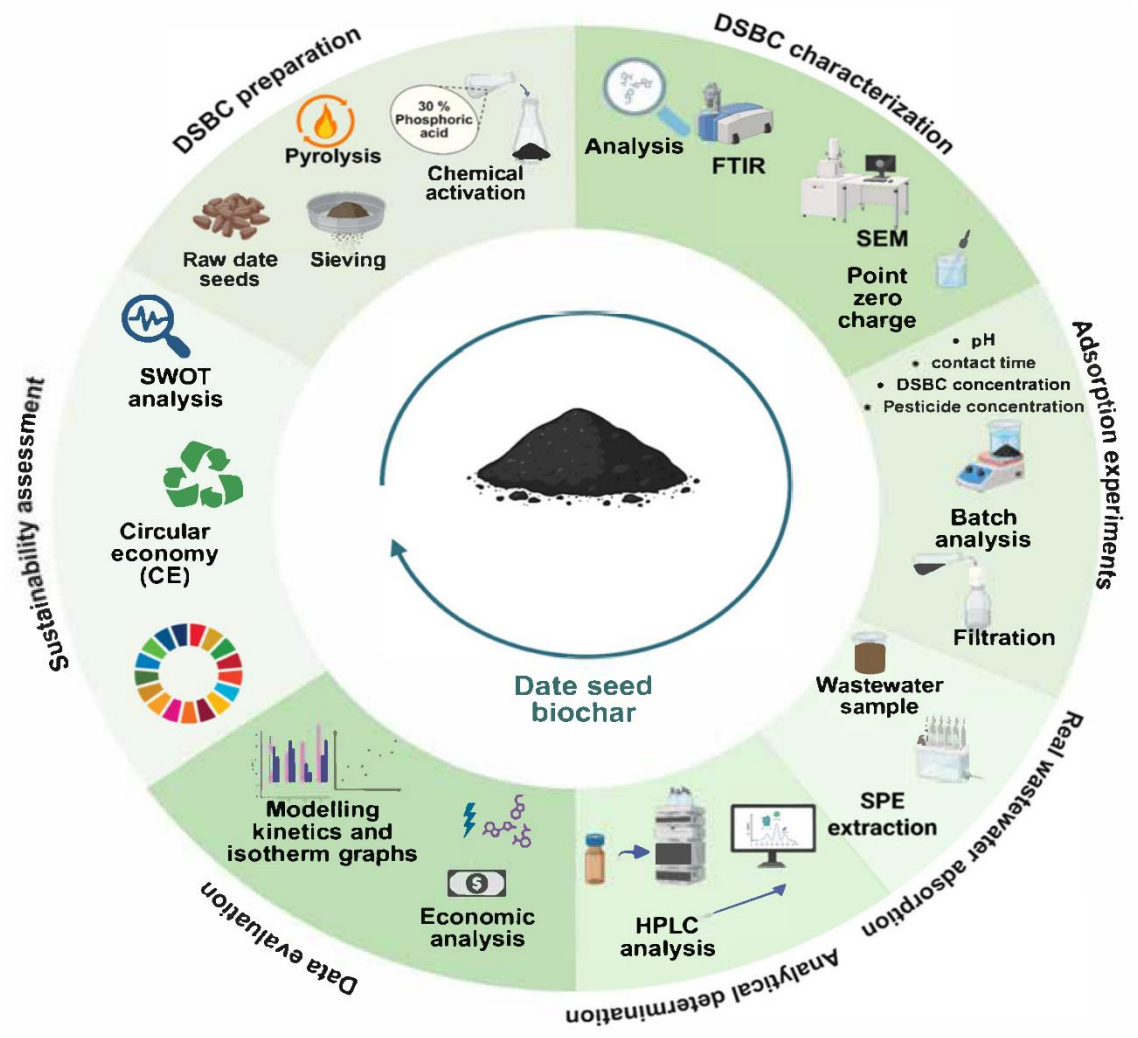

Figure 4. Conceptual framework for valorizing date seeds into biochar for pesticide removal. Reprinted from ref. [4]. Copyright (2025), with permission from MDPI.

The adsorption of various contaminants from wastewater using biochar derived from various agricultural wastes is summarized in Table 3.

 doi:10.20944/preprints202510.1476.v1

Table 3. The adsorption of contaminants from wastewater using biochar derived from agricultural wastes.

Precursors of biochar	Pollutants	Wastewater	Fabrication conditions of biochar	Adsorption conditions	Surface area, pore size, total pore volume	Functional groups and mechanisms	Adsorption capacities	RE (%)	Refs.
Date seed	Carbendazim Linuron	Municipal wastewater	550°C, 0.5 h, N_2 atmosphere	3 g biochar/L, pH 7, 40 min, 200 mL, 1 mg/L	307.5 m^2/g, 3.80 nm, 0.278 cm^3/g	-OH, -COOH, -Ph π–π electron donor–acceptor interactions, π–π stacking, dipole–dipole interactions, pore filling, electrostatic attraction, H-bonding	-	88.7 85.9	[4]
Corncob	N, P, K	Human urine Biogas wastewater	600°C, anaerobic condition	60 g biochar, 600 mL, 5 days	1.7 m^2/g, -, 0.0005 cm^3/g	-OH, -COOH, C = C ion exchange, chemical interaction	1200, 242.8, 43.7 mg/L 342.4, 105, 35 mg/L	-	[11]
Groundnut shells, drumstick seeds, coconut fiber	BOD	Pharmaceutical wastewater	Groundnut shell: 500°C, 4 h; drumstick seeds: 600°C, 2 h; coconut fiber: 700°C, for 2 h	35 g biochar mixture (1:1:1), 443.6 mg/L, pH 7, 25°C, 1.5 h	-	OH, $-CH_3$, C-H, C=C, C-OH, C=O -	-	72.1	[7]
Coconut shells	Methylene blue	Dye wastewater	-	20 mg Fe_3O_4/biochar /sodium alginate aerogel beads, 50 mL, 50 mg/L, 150 rpm, 25°C, 24 h, pH 7	152.5 m^2/g, 2.60 nm, -	-OH, -COOH pro-filling, H-bonding, electrostatic interaction	-	-	[5]
Rice husk	TC N, P, K	Human urine	-	0.1 g biochar/mL, 5 days	4.63 m^2/g, -, -	–OH, C-H, C-O, C=C	- 236.5, 256.7, 4.6 mg/L	60-80 50, 70, 80	[12]

 doi:10.20944/preprints202510.1476.v1

						H-bonding, ligand exchange, ion exchange, electrostatic interactions			
Peanut shell	Atrazine	Synthetic wastewater	450°C, 4 h	20 mg biochar, 25 mL, 20 mg/L, 150 rpm	61.8 m^2/g, 1.96 nm, 0.03 cm^3/g	-OH, NH_2, C-O, C=O, C-H, C=C, C-C π-π interactions, H-bonding	2.8 mg/g	-	[6]
Coconut shell	Ammonium, nitrate, phosphate	Synthetic wastewater	-	0.5 g biochar, 100 mL, 80 mg/L, 6 h, 80 rpm	-	C=C, C-O-C, C=O ion exchange, chemical interaction	10.12, 7.51, 10.79 mg/g	-	[22]
Eucalyptus bar	Anthraquinon	Dye wastewater	500°C, 1.5 h, anaerobic condition	0.913 g biochar composite/L, 21 mg/L, pH 3.9, 117 min	57.4m^2/g, 1.48 nm, 0.41 cm^3/g	Si-OH, Si-N, -COOH, -OH, C-O-C, C=O π–π interaction, electrostatic attraction, surface functional groups, chemisorption, pore-filling	-	-	[50]
Walnut shell	Quinoline	Coking wastewater	500°C, 2 h, N_2 atmosphere	10 mg KOH-activated biochar, 50 mg/L, 25°C, 50 mL	969.8 m^2/g, 2.34 nm, 0.4 cm^3/g	C–O–C, C-O, C=OC-H, C-C, C=C–OH porous adsorption, π–π interaction, H-bonding, electrostatic attraction	78.2 mg/g	-	[59]
Giant reed	Basic blue 41	Textile wastewater	10 °C /min at 600°C for 2 h, 5 L/min of N_2 flow	4 g biochar/L, 5.7 mg/L, 1 h	429.0 m^2/g, -, 0.09 cm^3/g	C-H, C-O, C-C, C-OH, C=O, C=C electrostatic interactions	5.14 mg/L	90.3	[9]
	Color			4 g biochar/L, 106 Pt–Co, 1 h			83 Pt-Co	89.3	
	Turbidity			4 g biochar/L, 48.55 NTU, 1 h			33.7 NTU	69.4	
	COD			4 g biochar/L, 928 mg/L, 1 h			582 mg/L	62.7	
Mandarin tree pruning	Dissolved organics	Olive mill wastewater	600°C, N_2 atmosphere	5 g biochar, 6800 mg/L, 100 mL, 25°C, 160 rpm	-	- Precipitation, surface complexation,	-	28	[10]

 doi:10.20944/preprints202510.1476.v1

				1 g biochar, 17 g/L, 100 mL, 25°C, 160 rpm		electrostatic interactions, π–π interactions	140 mg/ g	-	
Eucalyptus wood	Anthracene	Vehicle-wash wastewater	450°C, 1 h, N_2 atmosphere	0.4 g biochar, 40 ppm, 1 h, pH 5, 50°C	18.4 m^2/g, 1.5 nm, 0.01 cm^3/g	C-H, C=C, C=O Van der Waals dispersive contacts, electrostatic interactions, H- H-bonding	-	98.4	[19]
Rice husks	Mn, Se, Fe ions	Urban wastewater	Biochar in 1 M NaOH ($m_{Biochar}/m_{NaOH}$, 2:1), 12 h, 25°C	0.25 g NaOH-biochar/, biochar/HCl-biochar, 0.303 mg/L Mn, 0.116 mg/L Se, 0.390 mg/L Fe, 50 mL, 200 rpm, 10 h	-	C≡C, C≡N, C=C,C-O, C-H, Si-O-Si electrostatic attraction, ion exchange, complexation, precipitation	-	76, 66, 66	[40]
			Biochar in 10% wt. HCl, 3 h, 500°C at 10 °C/min, 200, 8 h, mL/min of N_2 flow				-	30, 26, 59	
			350°C at 10 °C/min, 6 h, 200 mL/min of N_2 flow				-	3, 39, 48	
Garlic peel	Methylene blue	Industrial wastewater	150°C at 5 °C/min, 2 h, vacuum atmosphere	5 mg biochar, 20 mL, 50 mg/L, 1 h, 25°C	5.46 m^2/g, 1.49 nm, 0.18 cm^3/g	O-H, C=O, C-O, C=C-H Electrostatic attraction, H-bonding, π-π stacking	14.33 mg/g	-	[1]
Corn stover	Phosphate	Pig farm wastewater	500°C, 2 h, N_2 atmosphere	0.2 g Ce-modified biochar, 100 mL, 24 h, 180 rpm, 25°C	14.1 m^2/g, 7.05 nm, -	$-CH_2-$, -CH-, Ce-O surface precipitation, ligand exchange, complexation, electrostatic attraction	27.96 mg/g	43.3	[30]
Lotus leaf	Be ion	Simulated beryllium	600°C, 3 h	0.05 g PO_4^{3-}/NH_4^+ modified biochar, 50	4.927 m^2/g, 3.86 nm	Phosphoric acid, ammonia, -OH	40.38 g/kg	-	[71]

 doi:10.20944/preprints202510.1476.v1

		mining wastewater		mL, 35°C, pH 5.5, 16 h, 175 rpm		surface complexation and precipitation, pore filling,			
Palm leaves	Tetracycline	Synthetic wastewater	500°C, 2 h, 10 °C/min under N_2 atmosphere	1 g biochar/L, 20 mL, 0.5 mg/L, 180 rpm, pH 5.7, 24 h, 25°C	31.5 m^2/g, 5.38 nm, 0.03 cm^3/g	-COOH, -OH, C=O, C-O, C=C, C-H H-bonding, π-π interaction, electrostatic interaction, pore-filling	-	80	[2]
Prosopis juliflora	Sulfamethoxazole	Industry wastewater	600°C at 10 °C/min, 2 h, N_2 atmosphere	1 g biochar/L, pH 5, 5.3 mg/L, 2 h	875 m^2/g, -, -	-OH, -COOH, -Ph, C-N, C-H, C-Cl, C-O electrostatic interactions, H-bonding, π-π stacking	-	76.7	[57]
	Ciprofloxacin			1 g biochar/L, pH 5, 8.3 mg/L, 2 h				80.4	
	COD			1 g biochar/L, pH 5, 2.5 g/L, 2 h				79.4	
	TOC			1 g biochar/L, pH 5, 1.05 g/L, 2 h				88.2	
Oil palm fronds	COD	Latex industrial wastewater	300-438°C at 13 °C/min, 3 h	15 g Biochar/L, 4 h, 150 mL	68.98 m^2/g, 1.68 nm, -	O-H, C=C, C-H, C-O, S=O, Si-O-Si, S-S Ion exchange, H-bonding	-	41.2	[14]
	Suspended solids							87.6	
	Sulfate							58.8	
	Sulfide							56.8	
Bamboo	Phosphate	Phosphate Fertilizer Plant wastewater	900°C at 8 °C/min, 2 h, N_2 atmosphere	Iron/CaO-modified biochar, 1660 mg/L, 48 h	146.5 m^2/g, 2.78 nm, 0.1 cm^3/g	- Chemical precipitation	-	~100	[60]
Fronds and leaves of date palm	Phenol	Synthetic primary-treated wastewater	600°C at 8 °C/min, anaerobic condition	0.1 g biochar, pH 6, 20 h, 800 mg/L, 50 mL, 200 rpm	245.8 m^2/g, 4.6 nm, 0.12 cm^3/g	O-H, C=C, C-H, Si-O, -COOH π-π interactions, H-bonding, pore filling, electrostatic interaction	241 mg/g	60.3	[66]
		Synthetic secondary-treated wastewater		0.1 g biochar, pH 6, 20 h, 52 mg/L, 50 mL, 200 rpm			22.28 mg/g	85.7	
Parthenium hysterophorus	Cr ion	Tannery wastewater	500°C, 2 h	Fe_3O_4/biochar,85.13 mg/L	237.4 m^2/g, -, -	O-H, C-O-C, C-OH, Fe-O,	-	81.8	[39]

 doi:10.20944/preprints202510.1476.v1

						Van der Waals forces, H-H-bonding, hydrophobic interactions			
Corn straw	Cr ion	Industrial wastewater	500°C, 2 h, Ar atmosphere	0.05 g Fe_3O_4/biochar, 32.8 mg/L, 3 h, pH 6	508.4 m^2/g, 4.6 nm, 0.55 cm^3/g	Fe–O, Fe–OOH, C=O, O–H Surface physisorption, pore filling, and electrostatic interaction	-	72.6	[31]
Citrus trees	Tetracycline	Industrial wastewater	-	3.5 g biochar, 50 mL, pH 4, 90 mg/L, 20°C	364.9 m^2/g, 1.08 nm, 0.2 cm^3/g	O-H, C=C, C=O, C-H, C-Cl π-π interaction	-	95	[20]
Corncob	Ammonia	Livestock wastewater	450°C for 1.5 h, 4 °C/min	0.3 g, 50 mL, 6.2 mg/L pH 12, 1.5 h	-	-	-	83.98	[85]
Corn Stalks	COD	Hospital wastewater	400-500°C	56.0 mg/L	-	-	-	57.1	[29]
	BOD			46.8 mg/L				56.8	
Wheat straw	Inorganic-N	Simulated agricultural wastewater	450°C at 5 °C/min, 5 h, 400 mL/min of N_2 flow	10 g Mg-modified biochar/L, 24 h, 250 mL, 25°C, 80 rpm	23.4 m^2/g, -, 0.062 cm^3/g	C=C, -OH, -Ph -NH_2, -COOH H-bonding, π-π/n-π interaction	4.44 mg/g	-	[13]
Palm bunch	Methyl paraben	Secondary wastewater effluent	450°C at 10 °C/min, 0.5 h, 400 mL/min of N_2 flow	H_2SO_4-activated biochar	60.3 m^2/g, -, 0.54 cm^3/g	C=C, -OH, C=O, S=O, C≡C Channel diffusion, H bonding, Van der Waals force, n-π/π-π interaction	-	80.3	[86]
	Carbamazepine							79.9	
	Ibuprofen							70.2	
	Triclosan							74.3	
Rotten sugarcane bagasse	Pb ion	Stimulated wastewater	600°C, 2 h, air atmosphere	30 mg biochar, 50 mg/L, pH 5	391.9 m^2/g, 20.9 nm, 0.532 cm^3/g	-COOH, CHO, C=O, C-H, C=C, O-C=O Ion exchange, surface complexation/function group coordination, precipitation, π-π interaction	-	97.3	[51]
	Cu ion							99.8	
	Cr ion							100	
Wheat straw	COD	Dye industry wastewater	300-500°C	2.5 g biochar/L, 25 mL, pH 7.62, 150 rpm	-	C=C, C=O, C-H, C-O-C, -OH, -COOH	-	62	[24]

 doi:10.20944/preprints202510.1476.v1

						Ion exchange, Surface physisorption, electrostatic interaction, complexation			
Rice husk	Pb ion	Industrial wastewater	500°C at 5 °C/min, 2 h, N_2 atmosphere	Biochar, 35.7 mg/L, pH 6.68, 100 mL	63 m^2/g, -, 0.381 cm^3/g	C-H, C=O, -OH, C-O Ion exchange, surface physisorption, electrostatic interaction, complexation	-	63.8	[27]
Auricularia auricula spent substrate	Cd ion	Electroplating wastewater	500°C, 2 h, anoxic conditions	0.1 g CS_2-modified biochar/L, 5.21 mg/L Cd^{2+}, 1.11 mg/L Cu^{2+}, 48.72 mg/L Zn^{2+}, 25°C, pH 5.59, 2 h	2.54 m^2/g, 13.4 nm, 0.009 cm^3/g	C-S, -OH, S=C=S, C=O, -NH_2 Complexation, precipitation	14.01 mg/g	-	[52]
	Cu ion						13.56 mg/g		
	Zn ion						50.19 mg/g		
Coffee husk	Ammonium	Domestic wastewater	350°C, 1 h	20 g biochar/L, 130 rpm, 6 h, 108 mg/L, pH 7.4,	0.43 m^2/g, -, -	-OH, C-H, C=O, C=C, -COOH Complexation, ion exchange, H-bonding, electrostatic attraction	-	20	[47]
Maize stalk, black gram, pine needle, Lantana camara	COD	Municipal wastewater	600°C at 10 °C/min, 4 h	5 g steam-activated biochar, 5 days	38.9-43.9 m^2/g, 2.74-3.96 nm, 2.47-3.99 cm^3/g	-COOH, -OH, -NH_2 Electrostatic interaction, precipitation, surface complexation	-	88-91	[35]
	TSS							81-85	
	Ammonia							87-91	
	Total K&N							59-69	
	Total K							78-88	
	As ion							79-87	
	Cd ion							53-95	
	Cr ion							83-88	
	Pb ion							78-95	
	Zn ion							90-95	
	Cu ion							93-96	
Rice straw	COD	Livestock wastewater	300°C, 6 h	Batch mode, 4 g biochar/L, pH 9	35.4 m^2/g, -, 0.36 cm^3/g	- Polarity, hydrophobic/aromatic	-	40	[67]
	BOD			Batch mode, 4 g biochar/L, pH 9				40	

 doi:10.20944/preprints202510.1476.v1

	COD			Column mode, 373 mg/L COD, 105 min		interaction, and molecular size		79	
	BOD			Column mode, 240 mg/L BOD, 105 min				84	
Jujube seeds	TSS	Electroplating industrial wastewater	Jujube seeds/H_2SO_4, 1:3 for 4 h, sonication 20 min at 24 kHz	2 g biochar/L, pH 1 h, 30°C, 20 mg/L	48.32 m^2/g, -, 0.16 cm^3/g	-OH, C=C, C=O, C-OH, La-OP-, -CO= Ligand exchange, electrostatic attraction, complexation	-	10	[74]
	TDS			2 g biochar/L, pH 1 h, 30°C, 2.8 g/L				0.79	
	Ni ion			2 g biochar/L, pH 1 h, 30°C, 15 mg/L				99.9	
	Zn ion			2 g biochar/L, pH 1 h, 30°C, 20 mg/L				~100	
	Cu ion			2 g biochar/L, pH 1 h, 30°C, 40 mg/L				~100	
	Cr ion			2 g biochar/L, pH 1 h, 30°C, 70 mg/L				~100	
Coconut husk	NO_3-N and NO_2-N	Slaughterhouse wastewater	700°C, 6 h, under N_2 atmosphere	1.5 g biochar, 26°C, pH 7.35, 50 mL, 120 rpm, 2 h	6.84 nm	-OH, C=C, Si-O-Si ligand exchange, electrostatic attraction, complexation	0.2-13 mg/g	-	[74]
Rice husk					1.97 nm		0.2-12 mg/g		
Coffee husk					1.63 nm		0.2-12 mg/g		
Pomelo peel	Tetracycline	Synthetic swine wastewater	400°C at 10 °C/min, 2 h	80 mg KOH-activated biochar/L, 10 mg/L, pH 7, 21°C, 75 h	2457.4 m^2/g, -, 1.14 cm^3/g	C≡C, C≡N, C-C, C=C, C-H, C-O-C, C=O π-π electron donor–acceptor interaction, electrostatic interaction, pore filling	-	85.0	[41]
	Oxytetracycline							82.2	
	Chlortetracycline							96.6	
Corn straw	TS	Swine wastewater	500°C, 1 h, N_2 atmosphere	Biochar or NaOH-activated biochar, 10.6 g/L TS, 0.3 g/L TVSS, 2985.6,1908.2, 1270.3, 981.4, 85.7, 4138.6, 655.9, 0.6, 2.7, 1.1, 6.1, 0.5, and 0.2	-	- H-bonding, electrostatic attraction, ion exchange, hydrophobic interaction	-	50-42	[42]
	TVSS							67-67	
	TC							53-72	
	TOC							55-73	
	TN							18-33	
	NH_4^+-N							22-32	
	TP							19-25	
	COD							20-26	

 doi:10.20944/preprints202510.1476.v1

	K ion			mg/L for TC, TOC, TV, NH_4^+-N, TP, COD, K, Mg, Cu, Zn, Ca, Fe, and Mn, respectively				39-67	
	Mg ion							33-83	
	Cu ion							59-41	
	Zn ion							27-73	
	Ca ion							30-54	
	Fe ion							80-80	
	Mn ion							100	
Platanus balls	Phosphate	Actual wastewater	600°C at 10 °C/min, 2 h, N_2 atmosphere	Column mode, 1 g La-modified biochar	77.01 m^2/g	LaO-, O-PO-, P-O electrostatic adsorption, ligand exchange, complexation	14.85 g/g	-	[65]
Bagasse	Pb ion	Battery manufacturing industry wastewater	300°C, 2.5 h	5 g biochar, pH 5, 2.5 h, 25°C, 2.393 mg/L	12.38 m^2/g	C=O, C=C, C-H, C-N, -COO-, -COOH, -Ph-OH Complexation, ion exchange	12.74 mg/g	75.4	[56]
Potato peel	Cu ion	Industrial wastewater	450°C, 6 L/min of N_2 flow	0.25 g chitosan-modified biochar, 4 h	-	$-NH_2$	1.117 mg/L	-	[78]
	Pb ion					-	0.506 mg/L		

 doi:10.20944/preprints202510.1476.v1

As listed in Table 3, agricultural wastes, including waste date, corncob, corn straw, corn stalk, wheat straw, coir fiber, moringa oleifera seeds, groundnut shells, coconut shells and husk, coffee husk, rice husk and straw, eucalyptus bar, walnut shell, giant reed, mandarin tree pruning, eucalyptus wood, garlic peel, corn stove, lotus leaf, Prosopis juliflora, bamboo, bunch, fronds and leaves of date palm, Parthenium hysterophorus, citrus trees, rotten sugarcane bagasse, maize stalk, black gram, pine needle, lantana camara, jujube seeds, pomelo peel, platanus balls, bagasse, and potato peel have been used for the adsorption of different contaminants and nutrients from various wastewater, such as municipal wastewater, human urine, biogas wastewater, pharmaceutical wastewater, dye wastewater, cooking wastewater, textile wastewater, olive mill wastewater, Vehicle-wash wastewater, Urban wastewater, pig farm wastewater, tannery wastewater, livestock wastewater, hospital wastewater, electroplating wastewater, domestic wastewater, Slaughterhouse wastewater, swine wastewater, mining wastewater, industrial wastewater, and stimulated wastewater. The calcined temperature and duration for biomass carbonization are in the range of 300-90°C and 0.5-6.0 h, respectively, under N_2, Ar, or vacuum atmosphere, depending on the agricultural wastes. The specific surface area, pore diameter, and total pore volume of different pristine biochar range from 1.65 to 428.98 m^2/g, from 1.08 to 20.9 nm, and from 0.0005 to 0.532 cm^3/g, respectively. The activated biochar usually possesses better porosity and higher surface areas. Functional groups -OH, -COOH, C-H, C=C, and C=O are crucial for the effective adsorption of contaminants from various wastewater. The adsorption equilibrium duration lasts from 40 min to 5 days.

5. Economic Evaluation and Environmental Impacts

Owing to the high cost-effectiveness, adsorption ability, and large agricultural biomass reserves, biochar has been seen as an excellent alternative adsorbent for activated carbons [13,66]. Accordingly, biochar is ~6-fold cheaper compared to the majority of activated carbons (up to 9 $/kg) [40]. Compared to activated carbon, the production cost of wheat straw-based biochar is reduced by 34-fold [13]. The energy requirement for preparing biochar was reported to be 15-fold lower compared to activated carbon [13]. Another work states that the cost of biochar (0.08 $/kg) is 12 times lower than other C-based adsorbents[87]. Specifically, in the Philippines, the evaluated costs are 0.09 $/kg for plant-based biochar and 1.1-1.7 $/kg for activated carbons [2]. The costs of biochar prepared from coconut shells [88], pine wood [88], rotten sugarcane bagasse [51], and pomelo peel [41] are 0.8, 0.9, 2.4, and 9.8 $/kg, respectively. It has been reported that the biochar market share will reach 0.45 billion in US dollars by 2030 globally[60]. Furthermore, the evaluated cost for treating real antibiotic wastewater using biochar is in the range of 9-914 $/$m^3$ [20]. For treating livestock wastewater, the cost is expected to be as high as 61.6 thousands $/year [67]. By using agricultural wastes, optimizing the pyrolysis process for energy efficiency, and ensuring responsible management of the spent biochar, the environmental benefits of wastewater remediation can significantly outweigh the localized or production-related burdens.

The positive environmental impacts of the preparation of biochar using agricultural waste for wastewater remediation are: i) Preventing the decomposition or open burning of agricultural waste minimizes the release of greenhouse gases and other harmful air pollutants; ii) biochar is highly effective at adsorbing and immobilizing a wide range of water contaminants, including heavy metals, nutrients, and recalcitrant organic pollutants, favoring produce cleaner effluent, safeguarding aquatic ecosystems and human health; iii) the pyrolysis process converts the carbon in the agricultural biomass into a highly stable, recalcitrant form C in the biochar, while the used biochar is often co-disposed or applied to soil (where applicable and safe). This carbon is sequestered for centuries, acting as a carbon-negative technology; vi) even though the biochar preparation releases certain waste gases into the atmosphere, the total emission is much decreased compared to the direct incineration, and the good reusability and regeneration properties of biochar reduce the potential environmental impacts [41]. A sustainability assessment described that the preparation of wheat straw-based biochar decreased fossil depletion by 35% and human toxicity by 13% [13]; v) by

 doi:10.20944/preprints202510.1476.v1

substituting traditional chemical adsorbents or treatment methods, biochar application can indirectly reduce emissions associated with the production of those alternatives; vi) mitigating the pollution risk of soil induced by agricultural wastes. Nevertheless, the topic can pose several potential environmental issues, including: i) energy consumption. The pyrolysis process used to create biochar requires energy (heat), which, if derived from non-renewable sources (e.g., grid electricity or fossil fuels), can contribute to the value of Global Warming Potential and other environmental burdens; ii) air emissions. Improper pyrolysis conditions (e.g., low temperature, incomplete combustion) can lead to the release of volatile organic compounds (VOCs) and polycyclic aromatic hydrocarbons (PAHs), which are environmental and health concerns; iii) precursor transportation. The environmental impact of transporting bulky agricultural waste from its source to the biochar production facility can be significant, influencing overall CO2 emissions; iv) long-term/post-application Impacts. Although biochar initially immobilizes heavy metals, its aging in the environment can, under certain conditions (e.g., changes in pH or redox potential), lead to the slow release of contaminants back into the environment; v) Contaminants in Biochar. If the agricultural waste itself contains high levels of pollutants (e.g., heavy metals from contaminated soil or feed), these can become concentrated in the resulting biochar, limiting its safe use for subsequent soil application. These issues can be addressed via the valorization of the syngas generated during pyrolysis (e.g., to power the process), using higher temperature and well-controlled systems, locating facilities close to precursor sources, proper post-treatment disposal, and careful precursor selection, respectively.

6. Future Directions and Challenges

The future perspective of biochar derived from agricultural wastes for wastewater remediation is highly promising, positioning it as a key sustainable technology within the circular economy. This topic converts agricultural residues (a waste management problem) into a value-added adsorbent and provides a cost-effective, eco-friendly alternative to conventional, energy-intensive wastewater treatment methods. The future studies in this field should move beyond simple, pristine biochar to highly engineered, designer materials for specific contaminants and applications. For example, i) the advanced biochar modification to fabricate nanocomposites and the development of innovative biochar (*e.g.*, magnetic biochar) with great reusability, good recyclability, and easy separation from the adsorption systems; ii) the investigation of the fixed bed adsorption and promotion of the biochar's regeneration and recycling properties; iii) the chemical and physical activation utilizing chemical and physical activators to optimize the porosity and surface chemistry for targeted contaminants; iv) Developing 'intelligent' or 'smart' biochar that can adjust their properties (like surface charge) in response to environmental conditions (*e.g.*, pH), allowing for better contaminant retention in dynamic systems; v) Removal of emerging contaminants such as pharmaceuticals, pesticides, and microplastics, where traditional treatments often fall short; vi) recovering valuable resources like nutrients (N and P) and heavy metals from wastewater, turning a pollution problem into a resource opportunity; vii) Synergistic integrating biochar not just as a standalone adsorbent but within hybrid systems, for instance, microbial fuel cells (biochar can serve as an electrode material to enhance electricity generation and pollutant breakdown simultaneously), membrane bioreactors (using biochar as a component in membranes or as a pre-treatment to reduce fouling and improve effluent quality), and algal-biochar systems (utilizing biochar to support microalgae growth for enhanced bioremediation, CO_2 capture, and even biofuel production); viii) the estimation of the feasibility of the long-term use of biochar in biofilters; ix) the simultaneous adsorption, decomposition, and mineralization via biodegradation using bacterial-loaded biochar, photocatalysis or sonocatalysis using biochar as catalysts, and activation of peroxymonosulfate or persulfate for wastewater purification [6,8,26,39,89]; x) optimizing biochar production technologies through innovations in pyrolysis, gasification, and hydrothermal carbonization to improve energy efficiency, enhance scalability, and ensure consistent biochar quality from diverse agricultural feedstocks; xi) Integrating machine learning and Artificial Intelligence (AI) with biochar production and application to accurately predict material properties, optimize treatment systems, and manage

 doi:10.20944/preprints202510.1476.v1

regeneration/disposal; xii) establishing closed-loop systems where agricultural waste is converted to biochar, used in wastewater treatment, and then the spent biochar (rich in recovered nutrients/carbon) is safely reused as a soil amendment, further supporting sustainable agriculture; and xiii) The scale-up of the obtained lab-outcomes in pilot and industrial levels.

Several challenges should be overcome for scaling up and commercialization: i) Material variability. Establishing standardized protocols for biochar production, characterization, and quality control to ensure consistent performance; ii) Regeneration and disposal. Developing cost-effective and environmentally friendly regeneration methods (e.g., chemical, thermal, biological) for spent biochar to ensure its long-term reusability and prevent secondary pollution; iii) Scalability and cost. Reducing production and modification energy costs to make engineered biochar competitive with established commercial adsorbents like activated carbon on a large scale; iv) Long-term ecotoxicity. Conducting extensive long-term field studies and life cycle assessments to fully understand the environmental stability and potential ecological risks of modified biochar.

7. Conclusions

Herein, this review shows a state-of-the-art of the adsorption removal of contaminants from wastewater using biochar derived from agricultural waste. Adsorption purification of wastewater using biochar derived from agricultural waste has attracted much more attention and attempts from researchers worldwide. Abundant agricultural wastes were valorized for biochar production, which has been subsequently applied for both the effective decontamination and the recovery of useful compounds from various wastewater. Most biochar adsorbents have good adsorption performance and reusability for real wastewater treatment. Interestingly, quite a part work titles the investigation biochar adsorption with wastewater; however, these works actually have nothing to do with wastewater treatment. The further enrichment and scale-up of the investigation are essential for the real-world implementation of the agricultural waste-derived biochar decomposition for wastewater remediation.

Author Contributions: Pengyun Liu: Data curation, Writing - Original draft preparation, Investigation, Validation. Luisa Boffa: Investigation, Methodology, Supervision. Giancarlo Cravotto: Conceptualization, Methodology, Supervision, Writing - Reviewing and Editing, *etc.*

Acknowledgments: This research was supported by the University of Turin (RILOM2024).

Conflicts of Interest: The authors declare no conflicts of interest.

Abbreviations

The following abbreviations are used in this manuscript:

BET	Brunauer–Emmett–Teller
BOD	Biochemical oxygen demand
COD	Chemical oxygen demand
EDS	Energy-dispersive X-ray spectroscopy
FT-IR	Fourier-transform infrared spectroscopy
PFO	Pseudo-first order
pH_L	pH of liquids
pH_{pzc}	Point of zero charge
PSO	Pseudo-second order
SEM	Scanning electron microscopy
TC	Total organic carbon
TDS	Total dissolved solids
TGA	Thermogravimetric Analysis
TOC	Total organic carbon

 doi:10.20944/preprints202510.1476.v1

TS	The total solids
TSS	Total suspended solids
TVSS	Total volatile suspended solids
XPS	X-ray photoelectron spectroscopy
XRD	X-ray diffraction

References

1. Shi, T.-T.; Yang, B.; Hu, W.-G.; Gao, G.-J.; Jiang, X.-Y.; Yu, J.-G. Garlic Peel-Based Biochar Prepared under Weak Carbonation Conditions for Efficient Removal of Methylene Blue from Wastewater. *Molecules* **2024**, *29*, 4772, doi:10.3390/molecules29194772.
2. Alshakhs, F.; Gijjapu, D.R.; Aminul Islam, Md.; Akinpelu, A.A.; Nazal, M.K. A Promising Palm Leaves Waste-Derived Biochar for Efficient Removal of Tetracycline from Wastewater. *J Mol Struct* **2024**, *1296*, 136846, doi:10.1016/j.molstruc.2023.136846.
3. Gao, R.; Ding, S.; Liu, Z.; Jiang, H.; Liu, G.; Fang, J. Recent Advances and Perspectives of Biochar for Livestock Wastewater: Modification Methods, Applications, and Resource Recovery. *J Environ Chem Eng* **2024**, *12*, 113678, doi:10.1016/j.jece.2024.113678.
4. Mihajlović, I.; Hgeig, A.; Novaković, M.; Gvoić, V.; Ubavin, D.; Petrović, M.; Kurniawan, T.A. Valorizing Date Seeds into Biochar for Pesticide Removal: A Sustainable Approach to Agro-Waste-Based Wastewater Treatment. *Sustainability* **2025**, *17*, 5129, doi:10.3390/su17115129.
5. Fan, W.; Zhang, X. Magnetic Coconut Shell Biochar/Sodium Alginate Composite Aerogel Beads for Efficient Removal of Methylene Blue from Wastewater: Synthesis, Characterization, and Mechanism. *Int J Biol Macromol* **2025**, *284*, 137945, doi:10.1016/j.ijbiomac.2024.137945.
6. Wang, Y.; Chen, Y.; Wang, L.; Mo, Y.; Lin, X.; Gao, S.; Chen, M. Efficient Removal of Atrazine in Wastewater by Washed Peanut Shells Biochar: Adsorption Behavior and Biodegradation. *Process Biochemistry* **2025**, *154*, 22–34, doi:10.1016/j.procbio.2025.04.008.
7. Soundari, L.; Prasanna, K. Optimum Usage of Biochar Derived from Agricultural Biomass in Removing Organic Pollutant Present in Pharmaceutical Wastewater. *Sustainable Chemistry for the Environment* **2025**, *10*, 100259, doi:10.1016/j.scenv.2025.100259.
8. Liu, P.; Wu, Z.; Manzoli, M.; Cravotto, G. Magnetic Biochar Generated from Oil-Mill Wastewater by Microwave-Assisted Hydrothermal Treatment for Sonocatalytic Antibiotic Degradation. *J Environ Chem Eng* **2025**, *13*, 114996, doi:10.1016/j.jece.2024.114996.
9. Abdu, M.; Babaee, S.; Worku, A.; Msagati, T.A.M.; Nure, J.F. The Development of Giant Reed Biochar for Adsorption of Basic Blue 41 and Eriochrome Black T. Azo Dyes from Wastewater. *Sci Rep* **2024**, *14*, 18320, doi:10.1038/s41598-024-67997-5.
10. Masmoudi, M.A.; Abid, N.; Feki, F.; Karray, F.; Chamkha, M.; Sayadi, S. Study of Olive Mill Wastewater Adsorption onto Biochar as a Pretreatment Option within a Fully Integrated Process. *EuroMediterr J Environ Integr* **2024**, *9*, 621–635, doi:10.1007/s41207-024-00464-9.
11. Van Nguyen, Q.; Nguyen, K.M.; Nguyen, H.T.; Van Hoang, H.; Duong, T.D.; Dong, M.T.N.; Tran, H.T.M. Transforming Domestic Wastewater into Hydroponic Nutrients Using Corncob-Derived Biochar Adsorption. *J Soil Sci Plant Nutr* **2025**, *25*, 3708–3724, doi:10.1007/s42729-025-02362-7.
12. Van Nguyen, Q.; Nguyen, K.M.; Nguyen, H.T.; Duong, T.D.; Dong, M.N.T.; Tran, H.M.T.; Van Hoang, H. Evaluation of Adsorption and Desorption of Wastewater onto Rice Husk Biochar on the Course of Hydroponic Nutrient Production. *Biomass Convers Biorefin* **2025**, *15*, 18615–18628, doi:10.1007/s13399-024-06485-2.
13. Yu, Y.; Yang, B.; Petropoulos, E.; Duan, J.; Yang, L.; Xue, L. The Potential of Biochar as N Carrier to Recover N from Wastewater for Reuse in Planting Soil: Adsorption Capacity and Bioavailability Analysis. *Separations* **2022**, *9*, 337, doi:10.3390/separations9110337.
14. Sutarut, P.; Cheirsilp, B.; Boonsawang, P. The Potential of Oil Palm Frond Biochar for the Adsorption of Residual Pollutants from Real Latex Industrial Wastewater. *Int J Environ Res* **2023**, *17*, 16, doi:10.1007/s41742-022-00503-9.

15. Liu, P.; Wu, Z.; Lee, J.; Cravotto, G. Sonocatalytic Degrading Antibiotics over Activated Carbon in Cow Milk. *Food Chem* **2024**, *432*, 137168, doi:10.1016/j.foodchem.2023.137168.
16. Pengyun, lLiu Cavitational Technologies for the Removal of Antibiotics in Water and Milk. PhD, University of Turin: Turin, 2023.
17. Liu, P.; Wu, Z.; Cannizzo, F.T.; Mantegna, S.; Cravotto, G. Removal of Antibiotics from Milk via Ozonation in a Vortex Reactor. *J Hazard Mater* **2022**, *440*, 129642, doi:10.1016/j.jhazmat.2022.129642.
18. Liu, P.; Wu, Z.; Fang, Z.; Cravotto, G. Sonolytic Degradation Kinetics and Mechanisms of Antibiotics in Water and Cow Milk. *Ultrason Sonochem* **2023**, *99*, 106518, doi:10.1016/j.ultsonch.2023.106518.
19. Ilyas, M.; Liao, Y.; Xu, J.; Wu, S.; Liao, W.; Zhao, X. Removal of Anthracene from Vehicle-Wash Wastewater through Adsorption Using Eucalyptus Wood Waste-Derived Biochar. *Desalination Water Treat* **2024**, *317*, 100115, doi:10.1016/j.dwt.2024.100115.
20. Rizkallah, B.M.; Galal, M.M.; Matta, M.E. Characteristics of Tetracycline Adsorption on Commercial Biochar from Synthetic and Real Wastewater in Batch and Continuous Operations: Study of Removal Mechanisms, Isotherms, Kinetics, Thermodynamics, and Desorption. *Sustainability* **2023**, *15*, 8249, doi:10.3390/su15108249.
21. Chen, Y.; Cui, Z.; Ding, H.; Wan, Y.; Tang, Z.; Gao, J. Cost-Effective Biochar Produced from Agricultural Residues and Its Application for Preparation of High Performance Form-Stable Phase Change Material via Simple Method. *Int J Mol Sci* **2018**, *19*, 3055, doi:10.3390/ijms19103055.
22. Edwin, T.; Komala, P.S.; Mera, M.; Zulkarnaini, Z.; Jamil, Z. Coconut Shell Biochar as a Sustainable Approach for Nutrient Removal from Agricultural Wastewater. *Journal of Water and Land Development* **2025**, 177–184, doi:10.24425/jwld.2025.154261.
23. Konneh, M.; Wandera, S.M.; Murunga, S.I.; Raude, J.M. Adsorption and Desorption of Nutrients from Abattoir Wastewater: Modelling and Comparison of Rice, Coconut and Coffee Husk Biochar. *Heliyon* **2021**, *7*, doi:10.1016/j.heliyon.2021.e08458.
24. Tariq, M.; Ali Baig, S.; Shams, D.F.; Hussain, S.; Hussain, R.; Qadir, A.; Maryam, H.S.; Khan, Z.U.; Sattar, S.; Xu, X. Dye Wastewater Treatment Using Wheat Straw Biochar in Gadoon Industrial Areas of Swabi, Pakistan. *Water Conservation Science and Engineering* **2022**, *7*, 315–326, doi:10.1007/s41101-022-00144-1.
25. Hossain, N.; Nizamuddin, S.; Griffin, G.; Selvakannan, P.; Mubarak, N.M.; Mahlia, T.M.I. Synthesis and Characterization of Rice Husk Biochar via Hydrothermal Carbonization for Wastewater Treatment and Biofuel Production. *Sci Rep* **2020**, *10*, 18851, doi:10.1038/s41598-020-75936-3.
26. Huong, P.T.; Jitae, K.; Al Tahtamouni, T.M.; Le Minh Tri, N.; Kim, H.-H.; Cho, K.H.; Lee, C. Novel Activation of Peroxymonosulfate by Biochar Derived from Rice Husk toward Oxidation of Organic Contaminants in Wastewater. *Journal of Water Process Engineering* **2020**, *33*, 101037, doi:10.1016/j.jwpe.2019.101037.
27. Pham, T.H.; Chu, T.T.H.; Nguyen, D.K.; Le, T.K.O.; Obaid, S. Al; Alharbi, S.A.; Kim, J.; Nguyen, M.V. Alginate-Modified Biochar Derived from Rice Husk Waste for Improvement Uptake Performance of Lead in Wastewater. *Chemosphere* **2022**, *307*, 135956, doi:10.1016/j.chemosphere.2022.135956.
28. Hosseini, S.M.; Bojmehrani, A.; Zare, E.; Zare, Z.; Hosseini, S.M.; Bakhshabadi, H. Optimization of Antioxidant Extraction Process from Corn Meal Using Pulsed Electric Field-subcritical Water. *J Food Process Preserv* **2021**, *45*, doi:10.1111/jfpp.15458.
29. Walanda, D.K.; Anshary, A.; Napitupulu, M.; Walanda, R.M. The Utilization of Corn Stalks as Biochar to Adsorb BOD and COD in Hospital Wastewater. *International Journal of Design and Nature and Ecodynamics* **2022**, *17*, 113–118, doi:10.18280/ijdne.170114.
30. Lou, L.; Li, W.; Yao, H.; Luo, H.; Liu, G.; Fang, J. Corn Stover Waste Preparation Cerium-Modified Biochar for Phosphate Removal from Pig Farm Wastewater: Adsorption Performance and Mechanism. *Biochem Eng J* **2024**, *212*, 109530, doi:10.1016/j.bej.2024.109530.
31. Chu, T.T.H.; Nguyen, M.V. Improved Cr (VI) Adsorption Performance in Wastewater and Groundwater by Synthesized Magnetic Adsorbent Derived from Fe3O4 Loaded Corn Straw Biochar. *Environ Res* **2023**, *216*, 114764, doi:10.1016/j.envres.2022.114764.
32. Favre, F.; Slijepcevic, A.; Piantini, U.; Frey, U.; Abiven, S.; Schmidt, H.-P.; Charlet, L. Real Wastewater Micropollutant Removal by Wood Waste Biomass Biochars: A Mechanistic Interpretation Related to

Various Biochar Physico-Chemical Properties. *Bioresour Technol Rep* **2022**, *17*, 100966, doi:10.1016/j.biteb.2022.100966.

33. Chen, H.; Guo, H.; Jiang, D.; Cheng, S.; Xing, B.; Meng, W.; Fang, J.; Xia, H. Microwave-Assisted Pyrolysis of Rape Stalk to Prepare Biochar for Heavy Metal Wastewater Removal. *Diam Relat Mater* **2023**, *134*, 109794, doi:10.1016/j.diamond.2023.109794.
34. Wainaina, S.; Awasthi, M.K.; Sarsaiya, S.; Chen, H.; Singh, E.; Kumar, A.; Ravindran, B.; Awasthi, S.K.; Liu, T.; Duan, Y.; et al. Resource Recovery and Circular Economy from Organic Solid Waste Using Aerobic and Anaerobic Digestion Technologies. *Bioresour Technol* **2020**, *301*, 122778, doi:10.1016/j.biortech.2020.122778.
35. Das, S.K.; Ghosh, G.K.; Avasthe, R. Conversion of Crop, Weed and Tree Biomass into Biochar for Heavy Metal Removal and Wastewater Treatment. *Biomass Convers Biorefin* **2023**, *13*, 4901–4914, doi:10.1007/s13399-021-01334-y.
36. Liu, P.; Wu, Z.; Sun, Z.; Ye, J. Comparison Study of Naphthalene Adsorption on Activated Carbons Prepared from Different Raws. *Korean Journal of Chemical Engineering* **2018**, *35*, 2086–2096, doi:10.1007/s11814-018-0124-7.
37. Liu, P.; Wu, Z.; Ge, X.; Yang, X. Hydrothermal Synthesis and Microwave-Assisted Activation of Starch-Derived Carbons as an Effective Adsorbent for Naphthalene Removal. *RSC Adv* **2019**, *9*, 11696–11706, doi:10.1039/C9RA01386E.
38. Liu, P.; Wu, Z.; Barge, A.; Boffa, L.; Martina, K.; Cravotto, G. Determination of Trace Antibiotics in Water and Milk via Preconcentration and Cleanup Using Activated Carbons. *Food Chem* **2022**, *385*, 132695, doi:10.1016/j.foodchem.2022.132695.
39. Fito, J.; Abewaa, M.; Nkambule, T. Magnetite-Impregnated Biochar of Parthenium Hysterophorus for Adsorption of Cr(VI) from Tannery Industrial Wastewater. *Appl Water Sci* **2023**, *13*, 78, doi:10.1007/s13201-023-01880-y.
40. Collivignarelli, M.C.; Illankoon, W.A.M.A.N.; Milanese, C.; Calatroni, S.; Caccamo, F.M.; Medina-Llamas, M.; Girella, A.; Sorlini, S. Preparation and Modification of Biochar Derived from Agricultural Waste for Metal Adsorption from Urban Wastewater. *Water (Basel)* **2024**, *16*, 698, doi:10.3390/w16050698.
41. Cheng, D.; Ngo, H.H.; Guo, W.; Chang, S.W.; Nguyen, D.D.; Zhang, X.; Varjani, S.; Liu, Y. Feasibility Study on a New Pomelo Peel Derived Biochar for Tetracycline Antibiotics Removal in Swine Wastewater. *Science of The Total Environment* **2020**, *720*, 137662, doi:10.1016/j.scitotenv.2020.137662.
42. Yu, J.; Hu, H.; Wu, X.; Zhou, T.; Liu, Y.; Ruan, R.; Zheng, H. Coupling of Biochar-Mediated Absorption and Algal-Bacterial System to Enhance Nutrients Recovery from Swine Wastewater. *Science of The Total Environment* **2020**, *701*, 134935, doi:10.1016/j.scitotenv.2019.134935.
43. Díaz, B.; Sommer-Márquez, A.; Ordoñez, P.E.; Bastardo-González, E.; Ricaurte, M.; Navas-Cárdenas, C. Synthesis Methods, Properties, and Modifications of Biochar-Based Materials for Wastewater Treatment: A Review. *Resources* **2024**, *13*, 8, doi:10.3390/resources13010008.
44. Idris, M.O.; Yaqoob, A.A.; Ibrahim, M.N.M.; Ahmad, A.; Alshammari, M.B. Introduction of Adsorption Techniques for Heavy Metals Remediation. In *Emerging Techniques for Treatment of Toxic Metals from Wastewater*; Elsevier, 2023; pp. 1–18.
45. Wu, Z.; Sun, Z.; Liu, P.; Li, Q.; Yang, R.; Yang, X. Competitive Adsorption of Naphthalene and Phenanthrene on Walnut Shell Based Activated Carbon and the Verification *via* Theoretical Calculation. *RSC Adv* **2020**, *10*, 10703–10714, doi:10.1039/C9RA09447D.
46. Wu, Z.; Liu, P.; Wu, Z.; Cravotto, G. In Situ Modification of Activated Carbons by Oleic Acid under Microwave Heating to Improve Adsorptive Removal of Naphthalene in Aqueous Solutions. *Processes* **2021**, *9*, 391, doi:10.3390/pr9020391.
47. Vu, N.-T.; Do, K.-U. Insights into Adsorption of Ammonium by Biochar Derived from Low Temperature Pyrolysis of Coffee Husk. *Biomass Convers Biorefin* **2023**, *13*, 2193–2205, doi:10.1007/s13399-021-01337-9.
48. Egila, J.N.; Dauda, B.E.N.; Iyaka, Y.A.; Jimoh, T. Agricultural Waste as a Low Cost Adsorbent for Heavy Metal Removal from Wastewater. *Int J Phys Sci* **2011**, *6*, 2152–2157.
49. Ye, M.; Fang, Y.; Xiang, H.; Liu, H.; Yan, H.; Wang, B.; Lin, X.; Liang, J.; Qian, W. Preparation and Modification of Bagasse Biochar Unveiling Ofloxacin Wastewater Adsorption. *Environ Technol* **2022**, 1–12, doi:10.1080/09593330.2022.2152222.

50. Yusuff, A.S.; Popoola, L.T.; Ibrahim, I.S. Adsorptive Removal of Anthraquinone Dye from Wastewater Using Silica-Nitrogen Reformed Eucalyptus Bark Biochar: Parametric Optimization, Isotherm and Kinetic Studies. *J Taiwan Inst Chem Eng* **2025**, *166*, 105503, doi:10.1016/j.jtice.2024.105503.
51. Bai, X.; Zhang, M.; Niu, B.; Zhang, W.; Wang, X.; Wang, J.; Wu, D.; Wang, L.; Jiang, K. Rotten Sugarcane Bagasse Derived Biochars with Rich Mineral Residues for Effective Pb (II) Removal in Wastewater and the Tech-Economic Analysis. *J Taiwan Inst Chem Eng* **2022**, *132*, 104231, doi:10.1016/j.jtice.2022.104231.
52. Wang, G.; Yang, R.; Liu, Y.; Wang, J.; Tan, W.; Liu, X.; Jin, Y.; Qu, J. Adsorption of Cd(II) onto Auricularia Auricula Spent Substrate Biochar Modified by CS2: Characteristics, Mechanism and Application in Wastewater Treatment. *J Clean Prod* **2022**, *367*, 132882, doi:10.1016/j.jclepro.2022.132882.
53. Enaime, G.; Baçaoui, A.; Yaacoubi, A.; Lübken, M. Biochar for Wastewater Treatment—Conversion Technologies and Applications. *Applied Sciences* **2020**, *10*, 3492, doi:10.3390/app10103492.
54. Adewoye, T.L.; Ogunleye, O.O.; Abdulkareem, A.S.; Salawudeen, T.O.; Tijani, J.O. Optimization of the Adsorption of Total Organic Carbon from Produced Water Using Functionalized Multi-Walled Carbon Nanotubes. *Heliyon* **2021**, *7*, e05866, doi:10.1016/j.heliyon.2020.e05866.
55. Ghebrehiwot, H.; Fynn, R.; Morris, C.; Kirkman, K. Shoot and Root Biomass Allocation and Competitive Hierarchies of Four South African Grass Species on Light, Soil Resources and Cutting Gradients. *Afr J Range Forage Sci* **2006**, *23*, 113–122, doi:10.2989/10220110609485894.
56. Poonam; Bharti, S.K.; Kumar, N. Kinetic Study of Lead (Pb2+) Removal from Battery Manufacturing Wastewater Using Bagasse Biochar as Biosorbent. *Appl Water Sci* **2018**, *8*, 119, doi:10.1007/s13201-018-0765-z.
57. Ashebir, H.; Nure, J.F.; Worku, A.; Msagati, T.A.M. Prosopis Juliflora Biochar for Adsorption of Sulfamethoxazole and Ciprofloxacin from Pharmaceutical Wastewater. *Desalination Water Treat* **2024**, *320*, doi:10.1016/j.dwt.2024.100691.
58. Tang, G.; Mo, H.; Gao, L.; Chen, Y.; Zhou, X. Adsorption of Crystal Violet from Wastewater Using Alkaline-Modified Pomelo Peel-Derived Biochar. *Journal of Water Process Engineering* **2024**, *68*, 106334, doi:10.1016/j.jwpe.2024.106334.
59. Cui, Y.; Du, W.; Zhang, Y.; Hu, J.; Kang, W. Adsorption Characteristics and Removal Mechanism of Quinoline in Wastewater by Walnut Shell-Based Biochar. *Journal of Water Process Engineering* **2025**, *70*, 106980, doi:10.1016/j.jwpe.2025.106980.
60. Ou, W.; Lan, X.; Guo, J.; Cai, A.; Liu, P.; Liu, N.; Liu, Y.; Lei, Y. Preparation of Iron/Calcium-Modified Biochar for Phosphate Removal from Industrial Wastewater. *J Clean Prod* **2023**, *383*, 135468, doi:10.1016/j.jclepro.2022.135468.
61. Illankoon, W.A.M.A.N.; Milanese, C.; Karunarathna, A.K.; Liyanage, K.D.H.E.; Alahakoon, A.M.Y.W.; Rathnasiri, P.G.; Collivignarelli, M.C.; Sorlini, S. Evaluating Sustainable Options for Valorization of Rice By-Products in Sri Lanka: An Approach for a Circular Business Model. *Agronomy* **2023**, *13*, 803, doi:10.3390/agronomy13030803.
62. Jeyasubramanian, K.; Thangagiri, B.; Sakthivel, A.; Dhaveethu Raja, J.; Seenivasan, S.; Vallinayagam, P.; Madhavan, D.; Malathi Devi, S.; Rathika, B. A Complete Review on Biochar: Production, Property, Multifaceted Applications, Interaction Mechanism and Computational Approach. *Fuel* **2021**, *292*, 120243, doi:10.1016/j.fuel.2021.120243.
63. Ambaye, T.G.; Vaccari, M.; van Hullebusch, E.D.; Amrane, A.; Rtimi, S. Mechanisms and Adsorption Capacities of Biochar for the Removal of Organic and Inorganic Pollutants from Industrial Wastewater. *International Journal of Environmental Science and Technology* **2021**, *18*, 3273–3294, doi:10.1007/s13762-020-03060-w.
64. Kılıç, M.; Keskin, M.E.; Mazlum, S.; Mazlum, N. Hg(II) and Pb(II) Adsorption on Activated Sludge Biomass: Effective Biosorption Mechanism. *Int J Miner Process* **2008**, *87*, 1–8, doi:10.1016/j.minpro.2008.01.001.
65. Jia, Z.; Zeng, W.; Xu, H.; Li, S.; Peng, Y. Adsorption Removal and Reuse of Phosphate from Wastewater Using a Novel Adsorbent of Lanthanum-Modified Platanus Biochar. *Process Safety and Environmental Protection* **2020**, *140*, 221–232, doi:10.1016/j.psep.2020.05.017.

66. Fseha, Y.H.; Shaheen, J.; Sizirici, B. Phenol Contaminated Municipal Wastewater Treatment Using Date Palm Frond Biochar: Optimization Using Response Surface Methodology. *Emerg Contam* **2023**, *9*, 100202, doi:10.1016/j.emcon.2022.100202.
67. Lap, B.Q.; Thinh, N.V.D.; Hung, N.T.Q.; Nam, N.H.; Dang, H.T.T.; Ba, H.T.; Ky, N.M.; Tuan, H.N.A. Assessment of Rice Straw–Derived Biochar for Livestock Wastewater Treatment. *Water Air Soil Pollut* **2021**, *232*, 162, doi:10.1007/s11270-021-05100-8.
68. Wu, Z.; Liu, P.; Wu, Z.; Cravotto, G. In Situ Modification of Activated Carbons by Oleic Acid under Microwave Heating to Improve Adsorptive Removal of Naphthalene in Aqueous Solutions. *Processes* **2021**, *9*, 391, doi:10.3390/pr9020391.
69. Tan, K.L.; Hameed, B.H. Insight into the Adsorption Kinetics Models for the Removal of Contaminants from Aqueous Solutions. *J Taiwan Inst Chem Eng* **2017**, *74*, 25–48, doi:10.1016/j.jtice.2017.01.024.
70. Freundlich, H. Über Die Adsorption in Lösungen. *Zeitschrift für Physikalische Chemie* **1907**, *57U*, 385–470, doi:10.1515/zpch-1907-5723.
71. Zhao, X.; Wang, Q.; Sun, Y.; Li, H.; Lei, Z.; Zheng, B.; Xia, H.; Su, Y.; Ali, K.M.Y.; Wang, H.; et al. Beryllium Adsorption from Beryllium Mining Wastewater with Novel Porous Lotus Leaf Biochar Modified with PO43−/NH4+ Multifunctional Groups (MLLB). *Biochar* **2024**, *6*, 89, doi:10.1007/s42773-024-00385-4.
72. Amdeha, E. Biochar-Based Nanocomposites for Industrial Wastewater Treatment via Adsorption and Photocatalytic Degradation and the Parameters Affecting These Processes. *Biomass Convers Biorefin* 2024, *14*, 23293–23318.
73. Motasemi, F.; Afzal, M.T. A Review on the Microwave-Assisted Pyrolysis Technique. *Renewable and Sustainable Energy Reviews* **2013**, *28*, 317–330, doi:10.1016/j.rser.2013.08.008.
74. Gayathri, R.; Gopinath, K.P.; Kumar, P.S. Adsorptive Separation of Toxic Metals from Aquatic Environment Using Agro Waste Biochar: Application in Electroplating Industrial Wastewater. *Chemosphere* **2021**, *262*, 128031, doi:10.1016/j.chemosphere.2020.128031.
75. Yap, M.W.; Mubarak, N.M.; Sahu, J.N.; Abdullah, E.C. Microwave Induced Synthesis of Magnetic Biochar from Agricultural Biomass for Removal of Lead and Cadmium from Wastewater. *Journal of Industrial and Engineering Chemistry* **2017**, *45*, 287–295, doi:10.1016/j.jiec.2016.09.036.
76. Hassan, N.S.; Jalil, A.A.; Izzuddin, N.M.; Bahari, M.B.; Hatta, A.H.; Kasmani, R.M.; Norazahar, N. Recent Advances in Lignocellulosic Biomass-Derived Biochar-Based Photocatalyst for Wastewater Remediation. *J Taiwan Inst Chem Eng* **2024**, *163*, 105670, doi:10.1016/j.jtice.2024.105670.
77. Gao, L.; Goldfarb, J.L. Heterogeneous Biochars from Agriculture Residues and Coal Fly Ash for the Removal of Heavy Metals from Coking Wastewater. *RSC Adv* **2019**, *9*, 16018–16027, doi:10.1039/C9RA02459J.
78. Hussain, A.; Maitra, J.; Khan, K.A. Development of Biochar and Chitosan Blend for Heavy Metals Uptake from Synthetic and Industrial Wastewater. *Appl Water Sci* **2017**, *7*, 4525–4537, doi:10.1007/s13201-017-0604-7.
79. Lee, J.W.; Han, J.; Choi, Y.-K.; Park, S.; Lee, S.H. Reswellable Alginate/Activated Carbon/Carboxymethyl Cellulose Hydrogel Beads for Ibuprofen Adsorption from Aqueous Solutions. *Int J Biol Macromol* **2023**, *249*, 126053, doi:10.1016/j.ijbiomac.2023.126053.
80. Qiu, L.; Zheng, P.; Zhang, M.; Yu, X.; Abbas, G. Phosphorus Removal Using Ferric–Calcium Complex as Precipitant: Parameters Optimization and Phosphorus-Recycling Potential. *Chemical Engineering Journal* **2015**, *268*, 230–235, doi:10.1016/j.cej.2014.12.107.
81. Kumi, A.G.; Ibrahim, M.G.; Fujii, M.; Nasr, M. Petrochemical Wastewater Treatment by Eggshell Modified Biochar as Adsorbent: Atechno-Economic and Sustainable Approach. *Adsorption Science & Technology* **2022**, *2022*, doi:10.1155/2022/2323836.
82. Muzyka, R.; Misztal, E.; Hrabak, J.; Banks, S.W.; Sajdak, M. Various Biomass Pyrolysis Conditions Influence the Porosity and Pore Size Distribution of Biochar. *Energy* **2023**, *263*, 126128, doi:10.1016/j.energy.2022.126128.
83. Ezeonuegbu, B.A.; Machido, D.A.; Whong, C.M.Z.; Japhet, W.S.; Alexiou, A.; Elazab, S.T.; Qusty, N.; Yaro, C.A.; Batiha, G.E.-S. Agricultural Waste of Sugarcane Bagasse as Efficient Adsorbent for Lead and Nickel

 doi:10.20944/preprints202510.1476.v1

Removal from Untreated Wastewater: Biosorption, Equilibrium Isotherms, Kinetics and Desorption Studies. *Biotechnology Reports* **2021**, *30*, e00614, doi:10.1016/j.btre.2021.e00614.

84. Shruthi, S.; Vishalakshi, B. Hybrid Banana Pseudo Stem Biochar- Poly (N-Hydroxyethylacrylamide) Hydrogel and Its Magnetic Nanocomposite for Effective Remediation of Dye from Wastewater. *J Environ Chem Eng* **2024**, *12*, 112682, doi:10.1016/j.jece.2024.112682.
85. El Ouassif, H.; Gayh, U.; Ghomi, M.R. Biochar Production from Agricultural Waste (Corncob) to Remove Ammonia from Livestock Wastewater. *International Journal of Recycling of Organic Waste in Agriculture* **2024**, *13*, doi:10.57647/j.ijrowa.2024.1301.09.
86. Choudhary, V.; Philip, L. Sustainability Assessment of Acid-Modified Biochar as Adsorbent for the Removal of Pharmaceuticals and Personal Care Products from Secondary Treated Wastewater. *J Environ Chem Eng* **2022**, *10*, 107592, doi:10.1016/j.jece.2022.107592.
87. Yoder, J.; Galinato, S.; Granatstein, D.; Garcia-Pérez, M. Economic Tradeoff between Biochar and Bio-Oil Production via Pyrolysis. *Biomass Bioenergy* **2011**, *35*, 1851–1862, doi:10.1016/j.biombioe.2011.01.026.
88. Fdez-Sanromán, A.; Pazos, M.; Rosales, E.; Sanromán, M.A. Unravelling the Environmental Application of Biochar as Low-Cost Biosorbent: A Review. *Applied Sciences* **2020**, *10*, 7810, doi:10.3390/app10217810.
89. Thuan, D. Van; Chu, T.T.H.; Thanh, H.D.T.; Le, M.V.; Ngo, H.L.; Le, C.L.; Thi, H.P. Adsorption and Photodegradation of Micropollutant in Wastewater by Photocatalyst TiO2/Rice Husk Biochar. *Environ Res* **2023**, *236*, 116789, doi:10.1016/j.envres.2023.116789.